Cartilage microRNA dysregulation during the onset and progression of mouse osteoarthritis overlaps with patient disease candidates

Louise H.W. Kung[1], Varshini Ravi[2], Lynn Rowley[1], Constanza Angelucci[1], Amanda J. Fosang[1,3], Katrina M. Bell[1], Christopher B. Little[2] and John F. Bateman[1,4]

[1]Murdoch Childrens Research Institute, Parkville, Victoria 3052, Australia.

[2]Raymond Purves Bone and Joint Research Laboratories, Kolling Institute of Medical Research, University of Sydney, St Leonards, New South Wales 2065, Australia.

Departments of [3]Paediatrics and [4]Biochemistry and Molecular Biology, University of Melbourne, Parkville, Victoria 3052, Australia

Correspondence:

John F. Bateman, Murdoch Childrens Research Institute, Royal Children's Hospital, Flemington Road, Parkville, Victoria, 3052, Australia. Tel: +613 8341 6422. Email: john.bateman@mcri.edu.au.

Conflict of interest statement:

The authors have declared that no conflict of interest exists.

Keywords: Osteoarthritis, microRNAs, cartilage, subchondral bone, microarray, DMM

ABSTRACT

The regulatory interplay between the joint cartilage and subchondral bone (SCB) is known be important in osteoarthritis (OA) pathology. Thus, to explore the role of microRNAs in osteoarthritis, we conducted global microRNA microarray expression profiling on microdissected medial tibial cartilage and SCB in a mouse model of OA produced by medial meniscus destabilization (DMM). Compared to sham-operated mice, DMM-operated mice had characteristic cartilage degeneration, SCB sclerosis and osteophyte formation. miRNA expression profiling revealed no statistically significant dysregulation of SCB miRNAs between DMM and sham-operated mice. In contrast, 139 miRNAs were found to be differentially expressed in DMM cartilage at 1 or 6 weeks post-surgery. To prioritize OA-candidates, dysregulated miRNAs were filtered against miRNAs identified in human OA and then using paired miRNA:mRNA expression analysis we identified a cohort of down-regulated microRNAs (miR-15a/16, 26b, 30c, 98, 149, 210, 342, 140, Let-7e) with corresponding changes in predicted target transcripts. Comparisons with microRNA dysregulation in DMM mouse cartilage where aggrecan cleavage was genetically ablated demonstrated that all, except Let-7e, were independent of aggrecan breakdown, earmarking this cohort of microRNAs of relevance to the critical early stages of OA initiation.

INTRODUCTION

Osteoarthritis (OA) is the most prevalent of all joint diseases, causing considerable morbidity, healthcare burden and financial expenditure (1, 2). Although many OA-related molecular pathways have been described, the key triggering molecular events remain elusive and as a result there are currently no registered therapies that halt disease onset or progression, only those which attempt to manage the associated pain (3, 4). Thus, discovering key pathological pathways which may offer new targets for disease modifying therapies is a priority.

Articular cartilage degeneration is the characteristic feature of OA and it is accompanied by sclerosis of the underlying subchondral bone (SCB), formation of osteophytes, ligament and meniscal damage along with synovial hyperplasia and inflammation, ultimately resulting in complete joint "organ" failure (5). While cartilage degradation remains the hallmark of OA, it is clear that all joint tissues can contribute to the pathological process with the regulatory interplay between the cartilage and SCB thought to be of particular importance (6, 7). However, the molecular characteristics of the disease pathways both within, and between these tissues remains poorly characterized, highlighting the critical need to perform parallel molecular studies on articular cartilage and SCB during OA initiation and progression. microRNAs (miRNAs; miRs) are an important class of cellular regulators which act by modulating gene expression at the post-transcriptional level during numerous physiological and disease settings (8-10). miRNAs are a family of evolutionarily conserved small non-coding RNAs, of which more than 2500 mature miRNAs have been identified in human to date (www.mirbase.org; (11)). Mature miRNAs range from 21-25 nucleotides in length and are formed from larger precursor miRNAs termed primary miRNAs (or pri-miR). The pri-miR are then processed by ribonuclease-III (RNase III) Drosha-DGCR8 micro-processing complex and subsequently Dicer to liberate mature miRNAs which then associate with Argonaute family proteins to form an RNA-induced silencing complex (RISC). These RISC effector complexes

are then guided to target genes where base-pairing of the miRNA results in translational repression or mRNA decay of the target transcript (12-14).

miRNAs have been shown to play critical roles in chondrocyte proliferation and differentiation during skeletal growth, as cartilage specific ablation of *Dicer* in mice resulted in skeletal abnormalities, decreased chondrocyte proliferation and accelerated differentiation into hypertrophic chondrocytes (15), the latter of which is a key OA-response (16, 17). Moreover, early postnatal deletion of *Drosha* in articular chondrocytes resulted in increased cell death and decreased matrix proteoglycan content (18), both also key pathophysiological features of OA. These studies demonstrate the critical role of miRNAs globally in cartilage development, health and disease. An increasing number of specific miRNAs have been suggested as regulators of chondrocyte-driven processes central to OA pathology (*see Reviews* (19-24)) making miRNAs viable new candidates for therapeutic targets and clinical biomarkers. Discovering their role in OA pathogenic processes is an exciting new frontier in unravelling the molecular mechanisms of OA to develop new mechanistically based therapies.

In this study we explore miRNAs dysregulated in articular cartilage and underlying SCB during the early stages of disease initiation and progression in a mouse model where OA was surgically-induced via destabilisation of the medial meniscus (DMM). This mouse model allows the molecular interrogation of the early stages of disease not possible with patient tissues. Studying these early stages of the disease is pivotal as it represents a critical time when therapeutic intervention is expected to have the most potential to delay disease progression and improve patient outcomes. We identified miRNA dysregulation specifically in OA cartilage and compared our data with previous human OA studies. *In silico* target prediction analysis on paired miRNA:mRNA data identified miRNA candidates with targets directly relevant to human OA pathology. Furthermore, by comparing OA-related miRNA candidates in wild-type mice with their expression following DMM mice in which aggrecan breakdown was

genetically ablated, we were able to discriminate between miRNAs which are independent of, or dependent on, aggrecan breakdown to provide additional insights into the sequence of miRNA dysregulation in the onset and progression of disease. Our study describes for the first time potential miRNA regulators of the initiation and progression of OA cartilage degeneration, not only validating those that have been shown in end-stage human OA but also identifying novel miRNAs not previously been associated with OA, that may be useful therapeutic targets for this recalcitrant disease.

RESULTS

Histological characterization of articular cartilage and SCB of DMM and sham-operated mice

DMM surgery induced a post-traumatic OA pathology characterized by chondrocyte hypertrophy, progressive proteoglycan loss, structural damage and SCB sclerosis (Fig. 1) as previously reported (25, 26). Chondrocyte hypertrophy was increased at both 1 and 6 weeks ($p = 0.002$ and 0.004, respectively), but did not progress with time in DMM between 1 and 6 weeks (Fig. 1A). There was no change in proteoglycan loss in DMM compared with sham-operated joints at 1 week, but significant proteoglycan loss was observed in the DMM group with time ($p = 0.0002$) and in DMM versus sham at 6 weeks ($p = 0.0002$; Fig. 1B). Similarly, total cartilage structural damage scores did not differ between DMM and sham at 1 week, but scores increased with time in DMM ($p = 0.01$) and were greater in DMM versus sham at 6 weeks ($p = 0.0002$; Fig. 1C).

There was no difference in SCB sclerosis between surgeries at 1 week (Fig. 1D) but by week 6 there was significant sclerosis in DMM compared with sham ($p = 0.003$) and in DMM at 6 weeks compared with DMM at 1 week ($p = 0.038$). There was no osteophyte development at 1 week but at 6 weeks they had formed in DMM only, being larger ($p = 0.002$) and more

mature (p = 0.001) than sham (Fig. 1E&F). Osteophyte maturation from cartilage to bone also progressed with time in DMM joints (p=0.03).

miRNA expression profiling of osteoarthritic SCB tissue

To assess the role of miRNAs in early OA we performed miRNA microarray analyses on 1 and 6 week post sham and DMM SCB and cartilage samples. Of the 1,881 miRNAs represented on the Agilent microarrays, 490 miRNAs were detected above background in SCB samples. Following stringent statistical analysis as described previously (27), we did not observe any statistically significant differences in miRNA expression in SCB between DMM and sham surgeries at either 1 or 6 week time points (Fig. 2A,B). However, there were statistically significant miRNA expression changes with post-operative time in SCB tissues (Supplemental Table 1). 37 miRNAs were dysregulated between 1 and 6 week time points in SCB (adj.p.value < 0.05; Supplemental Table 3) demonstrating the sensitivity and confidence of the microarray approach to detect miRNA expression changes if present.

The SCB miRNA array data was independently verified in an additional cohort of mice by qPCR of a selection of miRNAs (Supplemental Fig. 1). While changes in expression with post-operative time were evident, no statistically significant differences in miRNA expression were observed in DMM versus sham comparisons for most miRNAs evaluated (Supplemental Fig. 1), thus confirming the microarray data. A subtle decrease in expression for miR-3473b in DMM vs sham at 1 week (p=0.03; Supplemental Fig. 1G) was revealed by qPCR, however this difference was lost by week 6.

Dysregulated miRNA expression in DMM-induced OA cartilage

438 miRNAs were detected above background in cartilage samples. Of these, 359 miRNAs (~80%) were also expressed in SCB, with the remaining 79 miRNAs exclusively expressed in

cartilage. In contrast to the SCB above, miRNA expression profiling revealed 122 and 74 miRNAs that were differentially expressed (adj.p.value < 0.05) in cartilage of DMM versus sham-operated mice at 1 and 6 weeks post-surgery, respectively (Supplemental Tables 2-3). Of those, 69 miRNAs were up-regulated with adj.p.value < 0.05 and 53 miRNAs were down-regulated with adj.p.value < 0.05 in 1 week DMM vs sham (Fig. 2C). At 6 weeks, 42 miRNAs were up-regulated with adj.p.value < 0.05 and 32 miRNAs were down-regulated with adj.p.value < 0.05 in DMM vs sham (Fig. 2D).

Further analysis also demonstrated temporal patterns of differential miRNA expression. Of the 139 miRNAs dysregulated in total during the 6 week study, 65 and 17 miRNAs were uniquely dysregulated at 1 and 6 weeks, respectively, signifying these as potentially involved in OA initiation (week 1) and the development of cartilage degeneration over the first 6 weeks. Additionally, a cohort of 57 dysregulated miRNAs were common to both 1 and 6 week time points in the array data (Fig. 3). Amongst this 57, 12 miRNAs were identified with a robust array fold change > 2.0 and adj.p.value < 0.05, including miR-6931-5p, miR-466i-5p, miR-3082-5p, miR-1187, miR-669n, miR-468-3p, miR-669l-5p, miR-669e-5p and miR-672-5p, miR-574-5p, miR-32-3p (Supplemental Tables 2-3). Moreover, of the 139 dysregulated in cartilage, 110 miRNAs were found to be expressed in SCB but not differentially regulated. The remaining 29 dysregulated miRNAs were found to be unique to cartilage. This segregation of differential expression indicates the presence of tissue specific dysregulation of miRNAs.

To prioritise miRNA candidates from the pool of 139 dysregulated miRNAs (either at 1 and/or 6 weeks) we employed a two-branched filtering approach outlined in Figure 3. We conducted further analyses with our full dataset by (A) comparing it with findings from available human OA miRNA studies and (B) performing paired miRNA:mRNA target prediction analysis. miRNAs with no mRNA target data available and/or that had not been

identified in the four human OA patient datasets examined were excluded for further validation in this current study.

Comparison of our dataset with previously published human OA cartilage studies

Several dysregulated miRNAs have been identified in human end stage OA-cartilage from previous expression profiling experiments (28-31). Differentially expressed miRNAs identified from these 4 independent studies were compared, with related miRNA family members allocated into the same group as they most likely target the same genes/pathways e.g. miR-15a-5p and miR-16-5p, miR-26a/b, miR-30b/c/d. Nonetheless, there was a striking lack of overlap with only 6 out of 50 miRNAs identified (miR-342-3p, miR-25, miR-22-3p, miR-23b, miR-26-5p, miR-30-5p) common between any of the human studies (Fig. 4A). However, of the 50 dysregulated human OA miRNAs, a group of 12 miRNAs (adj.p.value < 0.05 at either 1 or 6 weeks) overlapped with our current study (Fig. 4B). Importantly, 11 of these miRNAs had OA-regulated mRNA target data (see below).

Prediction of putative target genes by paired miRNA:mRNA expression analysis

To further drill down on functionally important OA miRNAs we performed a bioinformatics-based analysis to identify putative target genes regulated by all the miRNAs significantly differentially expressed in OA cartilage at 1 and 6 weeks post DMM (Table 1&2). We used the microRNA target prediction module within Ingenuity Pathway Analysis which utilises several computational algorithms (including TargetScan Human, Tarbase) to predict or display experimentally observed target genes. We took advantage of our previous global mRNA expression profiling of cartilage from DMM-operated WT mice (at the same 1 and 6 week time points) (16). The analysis paired the expression of miRNA with mRNA (targets) to filter

inversely expressed miRNA-mRNA predicted interactions, and prioritise the most differentially expressed target transcripts with relevance to OA pathology (Table 1&2).

mRNA target data was generated for 57 of the 139 differentially expressed miRNAs. As mentioned above, 11 of these miRNAs were also found to be dysregulated in human OA, further adding to their clinical relevance. Interestingly, *Ptgs2* (*Cox-2*) which was one of the most highly up-regulated genes in DMM cartilage (16), has been shown to be experimentally regulated by multiple miRNAs, including miR-98-5p, miR-26b-5p, miR-15a-5p/miR-16-5p and Let-7d-5p, all of which were statistically significantly down-regulated in DMM cartilage (Table 1&2). In addition, we identified other important miRNA-mRNA paired interactions potentially involved in OA pathological pathways, such as, miR-149-5p-IL-11/-NPR3/-TNFRSF12A/-LTBP2, miR-98-5p-NGF/-CHSY3/-PTGS2, miR-26b-5p-COL10A1/-PTGS2, miR-30c-5p-NPR3/-NT5E/-BMP7, miR-15a-5p-NPR3/-PTGS2, miR-342-3p-PDGFRA/-IL-11/BMP7 and miR-377-3p-NT5E (Table 1&2).

qPCR validation of miRNA candidates with human OA relevance and OA-regulated target data

The 11 miRNAs prioritized through our filtering strategy were tested by qPCR on additional biological replicates to further confirm dysregulation in OA (Fig. 5). Of these, 7 were confirmed as differentially regulated in DMM compared with sham at 1 and/or 6 week time points (miR-15/miR-16-5p, miR-26b-5p, miR-30c-5p, miR-98-5p, miR-149-5p, miR-210-3p and miR-342-3p). No statistically significant differences were observed for miR-107-3p, miR-185-5p and miR-223-3p (Fig. 5) and miR-377-3p was undetectable by qPCR (data not shown). Therefore, these miRNAs which had not validated in a larger cohort of mice were removed from the candidate list.

Although unchanged in the microarray data, we also examined the expression of miR-140 in this larger cohort as it is known to be an important cartilage-specific miRNA involved in maintaining cartilage homeostasis (32). qPCR analysis revealed a significant decrease in miR-140 expression in DMM-operated cartilage at both 1 and 6 weeks in comparison to sham controls (Fig. 5L-M), thus corroborating with previous findings in human OA cartilage (29, 31, 33). Let-7e-5p was also examined as it was previously shown to be an inverse biomarker in patients with knee or hip OA (34). Correspondingly, DMM operated mice showed a significant decrease in Let-7e-5p compared with sham mice at both 1 and 6 weeks (Fig. 5N).

Dysregulated miRNA expression independent and dependent on aggrecan breakdown

Finally, we interrogated the expression of our identified high-priority miRNA candidates, in mice carrying a knockin mutation in aggrecan which endows resistance to aggrecanase cleavage in the interglobular domain and protection from DMM-induced cartilage proteoglycan loss and subsequent structural damage (Jaffa; *Acan* p.374ALGS→374NVYS) (35). Identifying miRNAs dysregulated in both wild type and Jaffa DMM allowed us to discriminate between miRNAs which are independent of aggrecan breakdown with those that are not dysregulated in Jaffa DMM and thus dependent on the degradation of aggrecan. Interestingly, dysregulated candidate miRNAs were on-the-whole similarly dysregulated in Jaffa DMM mice (Fig. 6). miR-15a-5p, miR-16-5p, miR-26b-5p, miR-30c-5p, miR-98-5p, miR-210-3p, miR-342-3p and miR-140 were statistically significantly down-regulated in Jaffa DMM (Fig. 6) mice in a similar fashion as wild type DMM mice (Fig. 5). miR-149-5p was down regulated in Jaffa at 1 week but not 6 weeks.

Notably, the statistical down-regulation of Let-7e-5p in wild type DMM (Fig 5) was not observed in protected Jaffa DMM mice (Fig 6) either at 1 week ($p=0.09$) or 6 weeks ($p=0.24$). This suggests that Let-7e-5p is downstream of aggrecan degradation as cartilage

damage progresses at 6 weeks and may be at least partially dependent on aggrecan breakdown during early OA at 1 week.

DISCUSSION

In this study, we have profiled miRNA expression in cartilage and SCB tissue of early OA joints induced by DMM surgery with the aim of exploring novel OA disease mechanisms which could underpin new therapeutic strategies. DMM mice demonstrated both time-dependent (cartilage proteoglycan loss, structural damage, sclerosis, osteophytes) and independent (chondrocyte hypertrophy) OA pathology, replicating key pathological features of the human condition. Correspondingly, we observed changes in miRNA expression specifically in cartilage that mirrored the temporal changes of proteoglycan loss and structural damage (specific to 6 weeks DMM) and the static changes of chondrocyte hypertrophy (both 1 and 6 weeks DMM). Consistent with the early detection of chondrocyte hypertrophy, *Col10a1* was previously shown to be significantly up-regulated in 1 week DMM (16).

We found that in total 139 miRNAs were dysregulated in cartilage during the development of post-traumatic OA over 6 weeks. Interestingly, 122 of these dysregulated mRNAs (~88%) were identified prior to any significant aggrecan degradation or cartilage structural degeneration at 1 week DMM suggesting that significant miRNA dysregulation could be involved in the initiation of OA pathology. Importantly, we interrogated the expression of DMM-dysregulated candidate miRNAs in mice resistant to aggrecan cleavage in the IGD which prevents the release of the entire glycosaminoglycan-containing portion of aggrecan by aggrecanases. This allowed us to identify miRNA expression changes that are dependent on, versus those that are independent of, ADAMTS-driven aggrecanolysis. Most of the miRNAs examined were shown to be independent of aggrecan cleavage, consistent with the dysregulation of these miRNAs prior to signs of proteoglycan loss and structural damage

in wild type DMM-operated mice. This suggests that the differential expression of these miRNAs occurs not as a result of the inflammation induced by joint injury/surgery (equivalent in sham and DMM) but as a response to increased mechanical stress induced by DMM surgery and the acute-initiation of the OA process rather than the downstream consequences of aggrecan breakdown. While functional analysis of the targets of the dysregulated candidate miRNAs will be needed to tease out key miRNAs that relate to OA pathology, these miRNA candidates can be segregated into several cohorts to explore possible roles in the initiation of progression of cartilage damage in human OA.

To filter down our list of 139 miRNAs and prioritize candidate miRNAs for further validation we compared our dataset with current miRNA datasets from human OA (28-31). Notwithstanding, that our OA model coincides with early stage cartilage degeneration and the human samples are from end-stage disease cartilage, miRNAs common to both groups are thus likely to be important throughout the OA process. We identified a group of 12 dysregulated miRNAs of particular interest as they overlap with miRNAs that have also been identified as dysregulated in one or more human OA studies (28-31) - miR-15a/16-5p, miR-26-5p, miR-30-5p, miR-98-5p, miR-107-3p, miR-149-5p, miR-185-5p, miR-210-3p, miR-223-3p, miR-337-3p, miR-342-3p, miR-377-3p (Fig 4B). The striking lack of overlap between the studies (6 out of 50: none in all 4 and only 1 common to 3 of the studies) emphasizes the patient and pathological variability of available OA cartilage from clinical samples, which makes interpreting the significance of the human OA-miRNAs and prioritizing miRNAs from these functional studies difficult. Our studies which interrogate genetically matched samples from a clinically reproducible OA model overcome this problem and provides confidence these overlapping 12 miRNAs are representative of both early and late-stage OA. Importantly, when we conducted paired analysis of miRNA dysregulation with the parallel changes in mRNA expression in DMM cartilage (16), all but one of these 12 candidates (miR-337-3p) showed the

corresponding cartilage expression changes of predicted or experimentally determined mRNA targets, compatible with the direction of miRNA expression change (Fig. 3; Tables 1&2). The expression of these 11 miRNA candidates were then measured in a larger cohort, where the differential expression of 7 were validated (miR-15a/16-5p, miR-26b-5p, miR-30c-5p, miR-98-5p, miR-149-5p, miR-210-3p, miR-342-3p) as high priority miRNA OA disease candidates, along with miR-140 and Let-7e-5p which were identified as dysregulated in our qPCR analyses. Interestingly, all except for Let-7e-5p were similarly down-regulated in the protected Jaffa mouse, and therefore, were independent of aggrecan breakdown and early cartilage pathology, suggesting these may be crucial in the mechanisms initiating the pathological cascades that result in eventual cartilage destruction. Thus, miR-15a/16-5p, miR-26b-5p, miR-30c-5p, miR-98-5p, miR-149-5p, miR-210-3p, miR-342-3p and miR-140 offer important potential targets in a critical therapeutic window. While Let-7e-5p dysregulation is reliant on aggrecan degradation, at 6 weeks, it is down-regulated at 1 week in wild-type DMM and also shows a trend towards down-regulation at 1 week in Jaffa (albeit not statistically significant). It is also therefore of interest and as an early OA-related miRNA. Our data is consistent with a previous study showing Let-7e-5p is an inverse clinical biomarker of OA (34).

miR-15 and miR-16 are of particular interest. miR-15 and miR-16 form a family of related small non-coding RNAs clustered within 0.5kb in the human genome. Both miR-15a-5p and miR-16-5p were down regulated in OA cartilage at both 1 and 6 weeks DMM (Fig. 5). Numerous studies have found miR-16 to be differentially expressed in human OA cartilage and plasma samples (29, 36-38). SMAD3, which has important roles in cartilage development and inflammation, was identified as a target gene of miR-16 in human chondrocytes (36). Furthermore, Ptgs2 and Npr3, both highly up-regulated in OA cartilage, were identified as experimentally validated targets of miR-15/16 seed sequences (Table 2), and both genes are known to have important roles in cartilage homeostasis and OA pathological processes (16,

39). Collectively, miR-15 and miR-16 may represent miRNAs with the potential to contribute to OA initiation and progression. More work is needed to conclusively determine their role in OA pathogenesis.

The remaining high-priority miRNAs candidates common to human and mouse OA also have targets and functions relevant to OA pathology. Target prediction analysis revealed the up-regulation of *Col10a1* may be mediated by the significant down regulation of miR-26b-5p (Table 1), consistent with the early detection of chondrocyte hypertrophy (Fig. 1). Moreover, the inhibition of miR-26b-5p in IL-1β treated human chondrocytes resulted in the up-regulation of catabolic genes such as MMP-3, -9, -13 and Ptgs2 (40). It was particularly striking that Ptgs2 (Cox2) was identified as a common target between several other dysregulated candidate miRNAs (miR-98-5p, miR-26b-5p, miR-15a-5p and Let-7d-5p). Ptgs2/Cox2 is involved in the biosynthesis of prostaglandin E2 which is a major catabolic and inflammatory mediator of cartilage degradation. The therapeutic inhibition of Ptgs2 through the use of selective and non-selective inhibitors has been extensively tested in clinical trials for the management of pain and inflammation associated with OA (41-43). With varying degrees of effectiveness, and controversy surrounding the safe clinical use of cox-2 inhibitors for the management of OA, the importance of cox-2 still remains to be determined (41, 44, 45). Nevertheless, the regulation of Ptgs2 by several OA-dysregulated miRNAs identified in this study is of high interest and warrants further pre-clinical studies examining the importance of these miRNAs and their contribution to OA pathology.

Furthermore, several members of the miR-30 family have also been shown to be differentially expressed in human OA (29, 31, 46). Specifically, we demonstrated miR-30c-5p to be significantly down regulated in DMM cartilage, and IPA target analysis revealed Npr3 and NT5E as experimentally validated targets of miR-30c-5p (Table 1). Npr3 is known to induce catabolic responses via MEK/ERK signalling and it can also stimulate anabolic

activities via Erk1/2 in an attempt to maintain homeostatic function (39). NT5E encodes CD73, deficiency of which leads to tissue calcification and early onset OA in hands (47). miR-98-5p has also been linked to OA-relevant pathways and has been shown to have roles in inflammatory processes by modulating IL-1β mediated production of TNFα (28). Intriguingly, the down regulation of miR-98-5p has been associated with an increased rate of apoptosis in human chondrocytes and exogenous injection of miR-98 mimic into an OA rat model demonstrated promising therapeutic benefit (48). Conversely, another rat OA study reported contradicting findings of miR-98 over-expression leading to detrimental effects on chondrocyte apoptosis and cartilage integrity (49). More studies are needed to conclusively determine the functional role of miR-98. The expression of other pro-inflammatory cytokines (TNFα, IL1β and IL6) has been shown to be regulated by miR-149-5p, thus highlighting miR-149-5p as an important inflammatory mediator in OA pathogenesis (50). Similarly, miR-210-3p was found to have regulatory roles in inflammation/cytokine expression (51), and its over-expression in OA rats decreased inflammation by inhibiting the NF-kB pathway, reducing cytokine production, leading to anti-inflammatory and anti-apoptotic effects (52). Collectively, these studies suggest these candidate miRNAs may have catabolic and inflammatory roles and further studies are required to dissect out their importance and the disease mechanisms involved.

A cohort of 57 dysregulated miRNAs were common to both 1 and 6 week time points in the array data (Fig. 3). Amongst the 57, 12 miRNAs had a robust array fold change > 2.0 and adj.p.value < 0.05, these included miR-6931-5p, miR-466i-5p, miR-3082-5p, miR-1187, miR-669n, miR-468-3p, miR-669l-5p, miR-669e-5p and miR-672-5p, miR-574-5p, miR-32-3p (Supplemental Tables 2-3). These miRNAs were not considered for further analysis in the current study as they did not satisfy the criteria to pass through our filtering strategy (Fig.3). Although mRNA target prediction data was demonstrated for some of these miRNAs (data not

shown), to our knowledge they have not been previously associated with human OA. Additionally, of these novel OA-related miRNAs only two (miR-574-5p, miR-32-3p) have currently identified human orthologues (www.mirbase.org). miR-574 was up-regulated during the early phases of mesenchymal stem cell differentiation towards chondrocytes (53). Importantly, over-expression of miR-574 resulted in inhibition of aggrecan and type II collagen expression, both key pathological hallmarks of OA, via an RXRα-Sox9 feedback mechanism (53). miR-574 has also been shown to target members of the β-catenin/Wnt signalling pathway, which we know to be pathologically dysregulated in OA (16). miR-32 has been shown to inhibit cell proliferation and negatively regulate Sox9, a critical transcription factor involved in chondrocyte differentiation (54).

The relevance of the dysregulated miRNAs without human orthologues is unclear. Currently, there are 2588 mature miRNAs known in humans but new ones are continuously being discovered. New evidence has emerged suggesting that over 1000 novel human miRNAs are yet to be uncovered as sequencing of more tissues and advancing technology come into play (55). Accordingly, Crowe et al. performed deep sequencing to identify novel miRNAs in human OA cartilage (56). Novel candidate miRNAs were characterized and validated in human tissue panels, chondrogenesis, chondrocyte differentiation and cartilage injury models, which led to the identification of 3 novel miRNAs with possible functional roles in cartilage homeostasis and OA (56). Current studies suggest that we are only scraping the surface of miRNA biology and it is likely that more are to be discovered and annotated. Of the group of miRNAs lacking human counterparts but most significantly up-regulated in DMM cartilage, miR-6931-5p and miR-3082-5p have not been associated with OA previously and their roles are not well known. miR-466i-5p on the other hand has been suggested to have a role in controlling inflammation, through targeting the expression of inflammatory markers such as

Cox-2/Ptgs2 and iNOS in liver inflammation (57). The roles of these miRNAs specifically in OA also remains to be determined.

We profiled miRNA expression in the adjoining sclerotic SCB tissue as it is well known that cartilage and SCB have a dynamic relationship involving biochemical and molecular crosstalk between the two tissues (6, 7). However, we were unable to detect statistically significant dysregulation of miRNAs in DMM versus sham SCB tissue. Although ~ 80% of the total number of miRNAs expressed and dysregulated in cartilage were also found in SCB tissue, none of these were significantly differentially regulated in OA SCB. Collectively, this supports the notion that OA is associated with cartilage-specific regulation of common miRNAs rather than the regulation of cartilage-specific miRNAs.

The lack of differential expression in SCB samples was not simply due to lack of sensitivity of our profiling approach as statistically significant temporal changes in miRNA expression were evident. This clearly demonstrates the sensitivity of the microarrays to detect miRNA expression changes if present, highlighting the robustness of the dataset. In contrast with our findings, two studies have previously identified miRNA dysregulation in SCB tissue from human end-stage OA (28, 58). Both demonstrated differential expression of 30 miRNAs in human OA bone tissue isolated during total knee replacement operations. The obvious discrepancies between our studies (species, model, stage of disease progression) may account for the lack of commonality between our datasets. Patients undergoing total knee surgery represent end-stage OA and exhibit substantial SCB changes impacted by years of progressive OA. In comparison our studies were conducted over a 6 week time period and thus recapitulate a mild early pathology. Investigating later time points after DMM would confirm whether miRNA changes occur with advanced pathology, however therapeutic intervention at such late stage of disease would be limited from a disease modifying prospective. Furthermore, our experiments which involve a laser micro-dissection approach to isolate RNA from the SCB,

incorporates genetic material originating from the surrounding bone marrow as well as bone tissue. As a result, only a small percentage of that material may be affected by the disease and thus any pathological changes would be masked by whole tissue extracts. Nonetheless, our data suggest that miRNA dysregulation in the SCB is not a significant component of the pathophysiology of OA initiation and early progression in this model. The identification of miRNA dysregulation specifically in cartilage, and not SCB, highlights the importance of specific cartilage-driven processes in the pathogenesis of OA.

For the first time, we have described potential miRNA regulators of early OA initiation and progression that share common findings with end-stage human OA data and also novel miRNAs which have not been previously associated with OA. *In silico* and experimental data generated target prediction algorithms on paired miRNA:mRNA expression, identified interesting miRNA candidates with targets relevant to OA pathology. Importantly, our studies provide critical information on the role of miRNAs during the early stages of OA initiation and progression not possible with patient tissues. Studying the early stages of the disease is pivotal mechanistically and because it represents a critical time when therapeutic intervention is expected to have the most disease modifying outcome. This present work provides a robust platform and validated pool of high-priority OA-associated miRNAs. Further studies are required to determine the role of specific individual miRNAs and explore their use as therapeutic targets in OA disease initiation and progression.

MATERIALS AND METHODS

Animal models and induction of OA

The generation of mice resistant to aggrecanase cleavage in the aggrecan IGD (Jaffa mouse) has been previously described (35). Post-traumatic OA was surgically induced in 10-12 week old male wild type C57BL6 and Jaffa mice by bilateral destabilization of the medial meniscus

(DMM), as described previously (25, 59). Briefly, the medial menisco-tibial ligament was exposed (by medial parapatellar arthrotomy and intrapatellar fat pad elevation, without tissue resection) and transected with curved dissecting forceps by one surgeon (CBL). Bilateral sham-operations were also performed, where the medial menisco-tibial ligament was visualized but not transected. All joints were flushed with sterile saline to remove any blood prior to separate closure of the joint capsule (simple continuous 8/0 polyglactin 910), subcutaneous tissue (mattress suture 8/0 polyglactin 910) and skin (cyanoacrylate).

DMM and sham were co-housed with 2-5 animals/30×20×18cm individually-ventilated-cage with filter lids, provided with sterilized bedding and environmental enrichment, maintained at 21-22°C with a 12-hour light/dark cycle, and received water and complete pelleted food *ad libitum*. Mice received no post-operative medication, were maintained in their pre-operative groups and were allowed unrestricted cage exercise.

Mice were randomly allocated to groups/harvest time point prior to study commencement using their individual ID numbers. Animals were sacrificed at 1 and 6 weeks after surgery. For each animal, one joint was processed for histology whilst the other was used for microarray expression profiling/qPCR. Microarray experiments on cartilage samples were performed on n = 3/group/time point, each consisting of RNA pooled from 3 individual mice. qPCR validation was performed on the same 3 pooled RNA samples and 4 additional biological replicates per time point per group. Microarray experiments on SCB samples were performed on n = 4/group/time point with qPCR validation performed on a different cohort of 4 mice/group/time point.

Histopathological analysis of OA features

Knee joints were dissected, fixed, decalcified, processed for histology and scored for OA histopathologic features as described previously (25). Sagittal sections every 80 μm across the

medial femoro-tibial joint were collected and stained with toluidine blue and fast green. Cumulative scores (total in all sections) of cartilage and SCB OA histopathologic features, which were determined by two independent observers (VR and CBL) who were blinded with regard to surgical intervention and post-operative time, were averaged, and these mean values provided a single histologic score for each of the following features in each mouse: cartilage proteoglycan loss (score range 0-3), structural damage (score range 0-7), chondrocyte hypertrophy (score range 0-1), SCB sclerosis (score range 0-3), osteophyte size (score range 0-3) and maturity (score range 0-3). Only histologic scores for the tibia are presented since miRNA profiling was performed on tibial articular cartilage only and can be correlated with adjacent SCB pathologic changes.

Laser capture micro-dissection and RNA preparation

Joint dissection, laser micro-dissection and RNA extraction from mouse cartilage and SCB was performed in a similar fashion to previously described (16, 60). Briefly, mice were sacrificed 1 and 6 weeks after surgery and the tibial epiphyses were isolated and placed in RNA Later (Life Technologies) containing 10% EDTA for at least 72 hrs at 4°C. After decalcification the samples were washed in DEPC-treated PBS, embedded in OCT and stored at -80°C. Serial 10 µm sagittal cryo-sections were fixed in ethanol and air-dried. Sections of the cartilage and underlying SCB of the medial tibial plateau were laser micro-dissected (Arcturus Bioscience) and collected. Total RNA was extracted from pooled laser micro-dissected sections from each individual mouse joint using TRIzol according to the manufacturer's instructions. RNA integrity and quantification was determined by capillary electrophoresis on a TapeStation 2200 with a high sensitivity screentape (Agilent Technologies) according to the manufacturer's specifications.

miRNA expression profiling

miRNA expression profiling was performed using SurePrint mouse miRNA microarray technology, release 21 (G4859C, Agilent Technologies) at the Ramaciotti Centre for Genomics (UNSW, Sydney, Australia). Briefly, 70 - 100 ng of total RNA was labelled and hybridized using the miRNA microarray System with miRNA complete labelling and Hyb kit version 3.0 (Agilent Technologies) by following manufacturer's instructions. The arrays were scanned on a G2565CA microarray scanner and the features were extracted using Agilent Feature Extraction 12.0.07 software. Bioinformatic analysis was performed by uploading paired miRNA:mRNA expression data (16) into the MicroRNA Target Filter module within Ingenuity Pathway Analysis (IPA, Qiagen Redwood City, CA, USA) application to generate a network of predicted miRNA gene targets directly relevant to OA cartilage.

Quantitative polymerase chain reaction (qPCR)

qPCR validation was carried out on a LightCycler 480 Instrument (Roche) using the miScript microRNA RT qPCR system (Qiagen) for miRNA expression by following manufacturer's instructions. All qPCR reactions were performed in duplicate and U6 snRNA and 5s rRNA were used as internal reference controls.

Statistical analysis

Comparison of histopathology scores between treatment groups and time points were analysed using nonparametric ranked Kruskal-Wallis analysis for multiple groups, and where there was significance ($p<0.05$) the Mann Whitney U-test (for unpaired data) was performed for between group comparisons with Benjamini-Hochberg correction for multiple comparisons applied (StatSE software, Stata corporation, TX, USA).

The microarray data was background corrected using the Normexp method and normalized with cyclic loess as previously described (27) using the bioconductor package Limma (Limma_3.20.9; (61)). Only probes with 10% greater signal than the negative controls in at least 4 samples were maintained for differential expression analysis. Probes were summarized initially at the probe level then at the gene level using the Limma avereps function, with control probes removed. Differential expression was assessed using moderated t-tests from the limma package. Results were adjusted for multiple testing using Benjamini-Hochberg method to control for false discovery rate. The data has been submitted to the GEO data repository (https://www.ncbi.nlm.nih.gov/geo/; accession number in progress).

miRNA qPCR expression data was quantitated using the comparative Ct method and the results were analyzed by nonparametric unpaired Mann-Whitney U-test to evaluate differences between group comparisons (GraphPad Prism, version 7.01).

Study approval

All animal procedures were approved by the Royal North Shore Hospital Animal Ethics Committee (Protocol RESP/14/77).

AUTHOR CONTRIBUTIONS

Conception and design: JFB, CBL

Collection and assembly of data: VR, LHK, LR, CA

Analysis and interpretation of the data: LHK, KMB, JFB, CBL

Providing reagents: AF

Drafting of the article: LHK, KMB, JFB, CBL

Critical revision of the article for important intellectual content: All authors

Final approval of the article: All authors

Obtaining of funding: JFB, CBL

ACKNOWLEDGMENTS

Supported by the National Health and Medical Research Council of Australia Project Grant APP1063133 and by the Victorian Government's Operational Infrastructure Support Program. The authors thank Ms Susan Smith for processing and sectioning the mouse knee joints, and blinding and randomising sections for scoring.

REFERENCES

1. Cross M, Smith E, Hoy D, Nolte S, Ackerman I, Fransen M, Bridgett L, Williams S, Guillemin F, Hill CL, et al. The global burden of hip and knee osteoarthritis: estimates from the global burden of disease 2010 study. *Ann Rheum Dis.* 2014;73(7):1323-30.
2. Puig-Junoy J, and Ruiz Zamora A. Socio-economic costs of osteoarthritis: A systematic review of cost-of-illness studies. *Seminars in Arthritis and Rheumatism.* 2015;44(5):531-41.
3. Hunter DJ. Pharmacologic therapy for osteoarthritis--the era of disease modification. *Nat Rev Rheumatol.* 2011;7(1):13-22.
4. Yu SP, and Hunter DJ. Managing osteoarthritis. *Australian Prescriber.* 2015;38(4):115-9.
5. Loeser RF, Goldring SR, Scanzello CR, and Goldring MB. Osteoarthritis: a disease of the joint as an organ. *Arthritis & Rheumatism.* 2012;64(6):1697-707.
6. Yuan XL, Meng HY, Wang YC, Peng J, Guo QY, Wang AY, and Lu SB. Bone-cartilage interface crosstalk in osteoarthritis: potential pathways and future therapeutic strategies. *Osteoarthritis Cartilage.* 2014;22(8):1077-89.
7. Sharma AR, Jagga S, Lee SS, and Nam JS. Interplay between cartilage and subchondral bone contributing to pathogenesis of osteoarthritis. *Int J Mol Sci.* 2013;14(10):19805-30.
8. Kloosterman WP, and Plasterk RH. The diverse functions of microRNAs in animal development and disease. *Dev Cell.* 2006;11(4):441-50.
9. Sayed D, and Abdellatif M. MicroRNAs in development and disease. *Physiol Rev.* 2011;91(3):827-87.
10. Lewis MA, and Steel KP. MicroRNAs in mouse development and disease. *Semin Cell Dev Biol.* 2010;21(7):774-80.

11. Kozomara A, and Griffiths-Jones S. miRBase: annotating high confidence microRNAs using deep sequencing data. *Nucleic acids research.* 2014;42(D1):D68-D73.

12. He L, and Hannon GJ. MicroRNAs: small RNAs with a big role in gene regulation. *Nat Rev Genet.* 2004;5(7):522-31.

13. Ameres SL, and Zamore PD. Diversifying microRNA sequence and function. *Nature reviews Molecular cell biology.* 2013;14(8):475-88.

14. Ha M, and Kim VN. Regulation of microRNA biogenesis. *Nature reviews Molecular cell biology.* 2014;15(8):509-24.

15. Kobayashi T, Lu J, Cobb BS, Rodda SJ, McMahon AP, Schipani E, Merkenschlager M, and Kronenberg HM. Dicer-dependent pathways regulate chondrocyte proliferation and differentiation. *Proceedings of the National Academy of Sciences of the United States of America.* 2008;105(6):1949-54.

16. Bateman JF, Rowley L, Belluoccio D, Chan B, Bell K, Fosang AJ, and Little CB. Transcriptomics of wild-type mice and mice lacking ADAMTS-5 activity identifies genes involved in osteoarthritis initiation and cartilage destruction. *Arthritis and rheumatism.* 2013;65(6):1547-60.

17. Little CB, and Hunter DJ. Post-traumatic osteoarthritis: from mouse models to clinical trials. *Nature reviews Rheumatology.* 2013;9(8):485-97.

18. Kobayashi T, Papaioannou G, Mirzamohammadi F, Kozhemyakina E, Zhang M, Blelloch R, and Chong MW. Early postnatal ablation of the microRNA-processing enzyme, Drosha, causes chondrocyte death and impairs the structural integrity of the articular cartilage. *Osteoarthritis and cartilage / OARS, Osteoarthritis Research Society.* 2015;23(7):1214-20.

19. Miyaki S, and Asahara H. Macro view of microRNA function in osteoarthritis. *Nature reviews Rheumatology.* 2012;8(9):543-52.

20. Swingler TE, Wheeler G, Carmont V, Elliott HR, Barter MJ, Abu-Elmagd M, Donell ST, Boot-Handford RP, Hajihosseini MK, Munsterberg A, et al. The expression and function of microRNAs in chondrogenesis and osteoarthritis. *Arthritis and rheumatism.* 2012;64(6):1909-19.

21. Gibson G, and Asahara H. microRNAs and cartilage. *Journal of orthopaedic research : official publication of the Orthopaedic Research Society.* 2013;31(9):1333-44.

22. Trzeciak T, and Czarny-Ratajczak M. MicroRNAs: Important Epigenetic Regulators in Osteoarthritis. *Current genomics.* 2014;15(6):481-4.

23. Nugent M. MicroRNAs: exploring new horizons in osteoarthritis. *Osteoarthritis and cartilage / OARS, Osteoarthritis Research Society.* 2015.

24. Vicente R, Noel D, Pers YM, Apparailly F, and Jorgensen C. Deregulation and therapeutic potential of microRNAs in arthritic diseases. *Nature reviews Rheumatology.* 2015.

25. Jackson MT, Moradi B, Zaki S, Smith MM, McCracken S, Smith SM, Jackson CJ, and Little CB. Depletion of protease-activated receptor 2 but not protease-activated receptor 1 may confer protection against osteoarthritis in mice through extracartilaginous mechanisms. *Arthritis & rheumatology.* 2014;66(12):3337-48.

26. Shu CC, Jackson MT, Smith MM, Smith SM, Penm S, Lord MS, Whitelock JM, Little CB, and Melrose J. Ablation of Perlecan Domain 1 Heparan Sulfate Reduces Progressive Cartilage Degradation, Synovitis, and Osteophyte Size in a Preclinical Model of Posttraumatic Osteoarthritis. *Arthritis & Rheumatology.* 2016;68(4):868-79.

27. Kung L, Zaki S, Ravi V, Rowley L, Smith M, Bell K, Bateman J, and Little C. Utility of circulating serum miRNAs as biomarkers of early cartilage degeneration in animal models of post-traumatic osteoarthritis and inflammatory arthritis. *Osteoarthritis and Cartilage.* 2016.

28. Jones SW, Watkins G, Le Good N, Roberts S, Murphy CL, Brockbank SM, Needham MR, Read SJ, and Newham P. The identification of differentially expressed microRNA in osteoarthritic tissue that modulate the production of TNF-alpha and MMP13. *Osteoarthritis and cartilage / OARS, Osteoarthritis Research Society.* 2009;17(4):464-72.

29. Iliopoulos D, Malizos KN, Oikonomou P, and Tsezou A. Integrative microRNA and proteomic approaches identify novel osteoarthritis genes and their collaborative metabolic and inflammatory networks. *PloS one.* 2008;3(11):e3740.

30. Diaz-Prado S, Cicione C, Muinos-Lopez E, Hermida-Gomez T, Oreiro N, Fernandez-Lopez C, and Blanco FJ. Characterization of microRNA expression profiles in normal and osteoarthritic human chondrocytes. *BMC musculoskeletal disorders.* 2012;13(144.

31. Song J, Kim D, Lee CH, Lee MS, Chun C-H, and Jin E-J. MicroRNA-488 regulates zinc transporter SLC39A8/ZIP8 during pathogenesis of osteoarthritis. *J Biomed Sci.* 2013;20(31.

32. Miyaki S, Sato T, Inoue A, Otsuki S, Ito Y, Yokoyama S, Kato Y, Takemoto F, Nakasa T, Yamashita S, et al. MicroRNA-140 plays dual roles in both cartilage development and homeostasis. *Genes & Development.* 2010;24(11):1173-85.

33. Miyaki S, Nakasa T, Otsuki S, Grogan SP, Higashiyama R, Inoue A, Kato Y, Sato T, Lotz MK, and Asahara H. MicroRNA-140 is expressed in differentiated human articular chondrocytes and modulates IL-1 responses. *Arthritis and rheumatism.* 2009;60(9):2723-30.

34. Beyer C, Zampetaki A, Lin NY, Kleyer A, Perricone C, Iagnocco A, Distler A, Langley SR, Gelse K, Sesselmann S, et al. Signature of circulating microRNAs in osteoarthritis. *Ann Rheum Dis.* 2015;74(3):e18.

35. Little CB, Meeker CT, Golub SB, Lawlor KE, Farmer PJ, Smith SM, and Fosang AJ. Blocking aggrecanase cleavage in the aggrecan interglobular domain abrogates cartilage erosion and promotes cartilage repair. *The Journal of clinical investigation.* 2007;117(6):1627-36.

36. Lisong L, Jie J, Xianzhe L, Shuhua Y, Shunan Y, Wen Y, and Yukun Z. MicroRNA-16-5p Controls Development of Osteoarthritis by Targeting SMAD3 in Chondrocytes. *Current Pharmaceutical Design.* 2015;21(35):5160-7.

37. Murata K, Yoshitomi H, Tanida S, Ishikawa M, Nishitani K, Ito H, and Nakamura T. Plasma and synovial fluid microRNAs as potential biomarkers of rheumatoid arthritis and osteoarthritis. *Arthritis Res Ther.* 2010;12(3):R86.

38. Borgonio Cuadra VM, Gonzalez-Huerta NC, Romero-Cordoba S, Hidalgo-Miranda A, and Miranda-Duarte A. Altered expression of circulating microRNA in plasma of patients with primary osteoarthritis and in silico analysis of their pathways. *PloS one.* 2014;9(6):e97690.

39. Peake NJ, Hobbs AJ, Pingguan-Murphy B, Salter DM, Berenbaum F, and Chowdhury TT. Role of C-type natriuretic peptide signalling in maintaining cartilage and bone function. *Osteoarthritis and Cartilage.* 2014;22(11):1800-7.

40. Yin X, Wang JQ, and Yan SY. Reduced miR‐26a and miR‐26b expression contributes to the pathogenesis of osteoarthritis via the promotion of p65 translocation. *Molecular Medicine Reports.* 2017;15(2):551-8.

41. Mathew ST, Devi S G, Prasanth VV, and Vinod B. Efficacy and Safety of COX-2 Inhibitors in the Clinical Management of Arthritis: Mini Review. *ISRN Pharmacology.* 2011;2011(480291.

42. Laine L, White WB, Rostom A, and Hochberg M. COX-2 Selective Inhibitors in the Treatment of Osteoarthritis. *Seminars in Arthritis and Rheumatism.* 2008;38(3):165-87.

43. van Walsem A, Pandhi S, Nixon RM, Guyot P, Karabis A, and Moore RA. Relative benefit-risk comparing diclofenac to other traditional non-steroidal anti-inflammatory drugs and cyclooxygenase-2 inhibitors in patients with osteoarthritis or rheumatoid arthritis: a network meta-analysis. *Arthritis Research & Therapy.* 2015;17(1):66.

44. Fukai A, Kamekura S, Chikazu D, Nakagawa T, Hirata M, Saito T, Hosaka Y, Ikeda T, Nakamura K, Chung U-i, et al. Lack of a chondroprotective effect of cyclooxygenase 2 inhibition in a surgically induced model of osteoarthritis in mice. *Arthritis & Rheumatism.* 2012;64(1):198-203.

45. Katz JA. COX-2 Inhibition: What We Learned—A Controversial Update on Safety Data. *Pain Medicine.* 2013;14(suppl 1):S29-S34.

46. Li L, Yang C, Liu X, Yang S, Ye S, Jia J, Liu W, and Zhang Y. Elevated expression of microRNA-30b in osteoarthritis and its role in ERG regulation of chondrocyte. *Biomedicine & Pharmacotherapy.* 2015;76(94-9.

47. Ichikawa N, Taniguchi A, Kaneko H, Kawamoto M, Sekita C, Nakajima A, and Yamanaka H. Arterial Calcification Due to Deficiency of CD73 (ACDC) As One of Rheumatic Diseases Associated With Periarticular Calcification. *JCR: Journal of Clinical Rheumatology.* 2015;21(4):216-20.

48. Wang G-L, Wu Y-B, Liu J-T, and Li C-Y. Upregulation of miR-98 Inhibits Apoptosis in Cartilage Cells in Osteoarthritis. *Genetic Testing and Molecular Biomarkers.* 2016;20(11):645-53.

49. Wang J, Chen L, Jin S, Lin J, Zheng H, Zhang H, Fan H, He F, Ma S, and Li Q. MiR-98 promotes chondrocyte apoptosis by decreasing Bcl-2 expression in a rat model of osteoarthritis. *Acta Biochim Biophys Sin (Shanghai).* 2016;48(923-9.

50. Santini P, Politi L, Vedova PD, Scandurra R, and Scotto d'Abusco A. The inflammatory circuitry of miR-149 as a pathological mechanism in osteoarthritis. *Rheumatology international.* 2014;34(5):711-6.

51. Qi J, Qiao Y, Wang P, Li S, Zhao W, and Gao C. microRNA-210 negatively regulates LPS-induced production of proinflammatory cytokines by targeting NF-kappaB1 in murine macrophages. *FEBS letters.* 2012;586(8):1201-7.

52. Zhang D, Cao X, Li J, and Zhao G. MiR-210 inhibits NF-kappaB signaling pathway by targeting DR6 in osteoarthritis. *Scientific reports.* 2015;5(12775.

53. Guerit D, Philipot D, Chuchana P, Toupet K, Brondello JM, Mathieu M, Jorgensen C, and Noel D. Sox9-regulated miRNA-574-3p inhibits chondrogenic differentiation of mesenchymal stem cells. *PloS one.* 2013;8(4):e62582.

54. Xu JQ, Zhang WB, Wan R, and Yang YQ. MicroRNA-32 inhibits osteosarcoma cell proliferation and invasion by targeting Sox9. *Tumour biology : the journal of the International Society for Oncodevelopmental Biology and Medicine.* 2014;35(10):9847-53.

55. Friedländer MR, Lizano E, Houben AJ, Bezdan D, Báñez-Coronel M, Kudla G, Mateu-Huertas E, Kagerbauer B, González J, and Chen KC. Evidence for the biogenesis of more than 1,000 novel human microRNAs. *Genome biology.* 2014;15(4):1.

56. Crowe N, Swingler T, Le L, Barter M, Wheeler G, Pais H, Donell S, Young D, Dalmay T, and Clark I. Detecting new microRNAs in human osteoarthritic chondrocytes identifies miR-3085 as a human, chondrocyte-selective, microRNA. *Osteoarthritis and Cartilage.* 2016;24(3):534-43.

57. Saravanan S, Thirugnanasambantham K, Hanieh H, Karikalan K, Sekar D, Rajagopalan R, and Hairul Islam VI. miRNA-24 and miRNA-466i-5p controls inflammation in rat hepatocytes. *Cellular & molecular immunology.* 2015;12(1):113-5.

58. Prasadam I, Batra J, Perry S, Gu W, Crawford R, and Xiao Y. Systematic Identification, Characterization and Target Gene Analysis of microRNAs Involved in Osteoarthritis Subchondral Bone Pathogenesis. *Calcified Tissue International.* 2016;99(1):43-55.

59. Glasson SS, Blanchet TJ, and Morris EA. The surgical destabilization of the medial meniscus (DMM) model of osteoarthritis in the 129/SvEv mouse. *Osteoarthritis Cartilage.* 2007;15(9):1061-9.

60. Belluoccio D, Rowley L, Little CB, and Bateman JF. Maintaining mRNA integrity during decalcification of mineralized tissues. *PloS one.* 2013;8(3):e58154.

61. Ritchie ME, Phipson B, Wu D, Hu Y, Law CW, Shi W, and Smyth GK. limma powers differential expression analyses for RNA-sequencing and microarray studies. *Nucleic acids research.* 2015:gkv007.

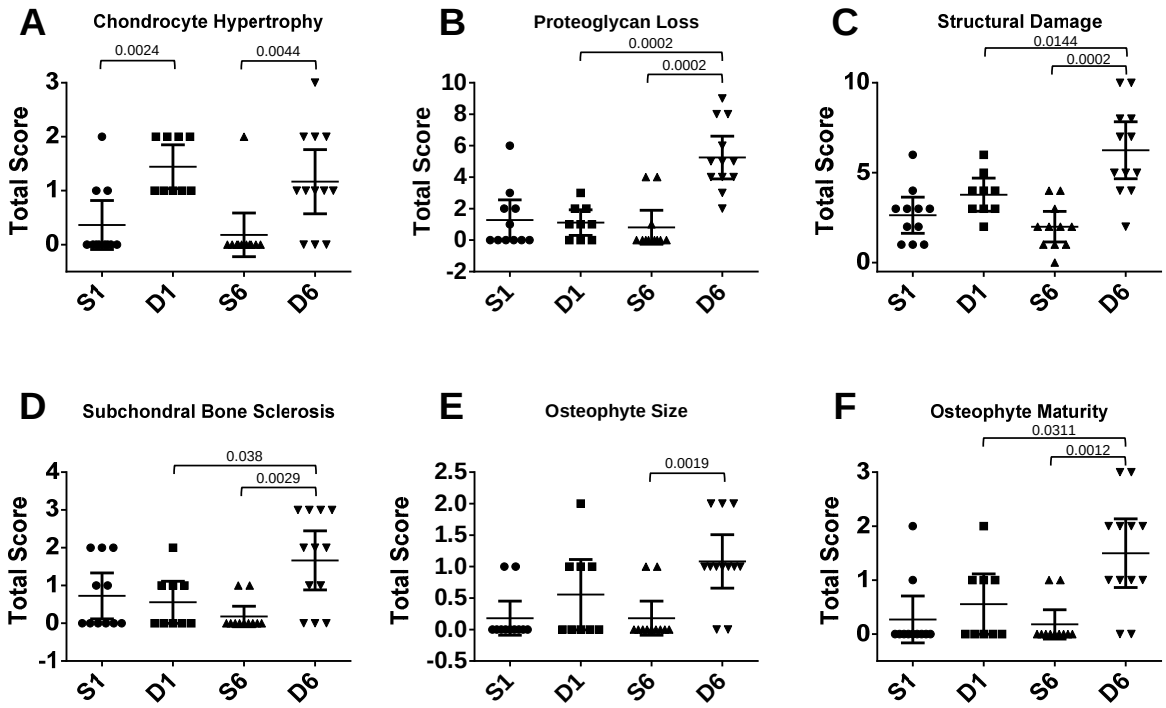

Figure 1. Cumulative histopathological scores of **(A)** chondrocyte hypertrophy, **(B)** cartilage proteoglycan loss, **(C)** articular cartilage structural damage, **(D)** subchondral bone sclerosis and osteophyte **(E)** size and **(F)** maturity in the proximal tibia of wild type sham and DMM operated knee joints at 1 and 6 weeks post surgery. Scatter plots display values for each individual mouse and mean (horizontal bar) ± 95% confidence intervals. Significant differences between groups connected by lines with exact p-values for each comparison indicated above the line, as determined by Mann-Whitney U-test with Benjamini-Hochberg multiple comparison correction. n = 11 (S1), n = 9 (D1), n = 11 (S6), n = 12 (D6). S = Sham; D = DMM.

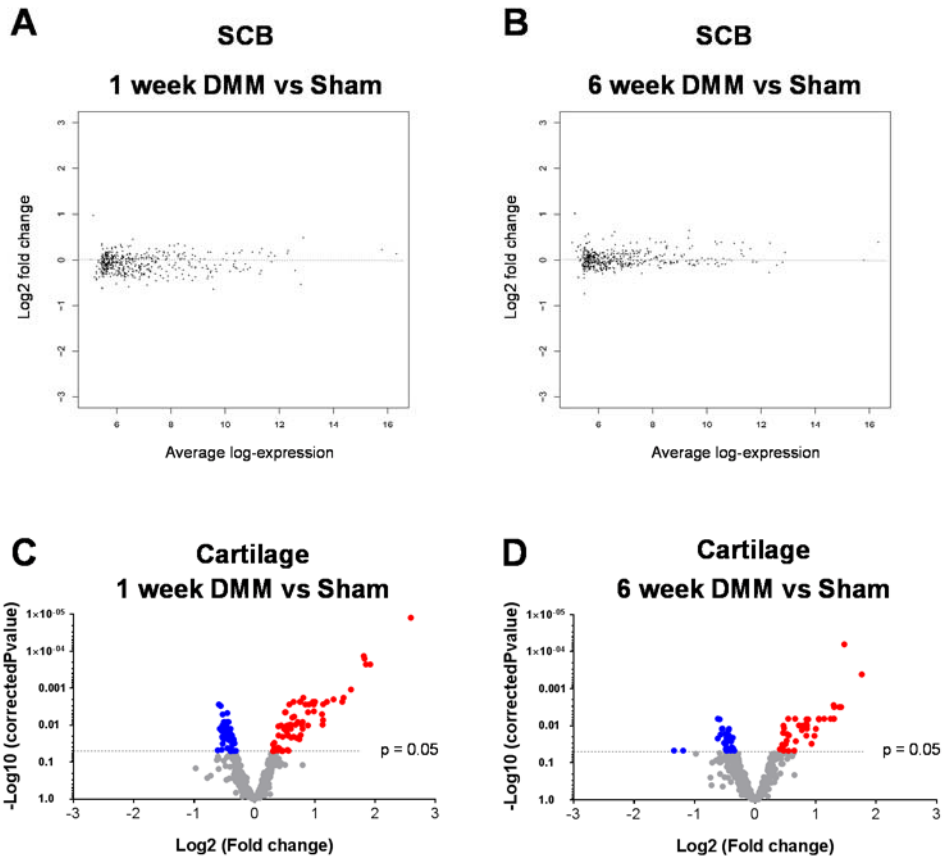

Figure 2. SCB and articular cartilage miRNA expression profiling. MA plots displaying average log-expression intensity values and log2 fold change for each miRNA expressed in SCB between DMM and sham in **(A)** 1 week and **(B)** 6 weeks. There were no significant changes in miRNA expression in SCB of DMM vs sham joints. Volcano plots showing differentially expressed miRNAs with adj.p-value < 0.05 in cartilage at **(C)** 1 and **(D)** 6 weeks post DMM vs sham. **(C)** 122 miRNAs were significantly dysregulated (adj.p-value < 0.05) in 1 week DMM vs sham (highlighted in blue+red). Of those, 69 miRNAs were up-regulated with adj.p-value < 0.05 (highlighted in red) and 53 miRNAs were down-regulated with adj.p-value < 0.05 (highlighted in blue) in 1 week DMM vs sham. **(D)** 74 miRNAs were significantly dysregulated (adj.p-value < 0.05) in 6 week DMM vs sham adj.p-value < 0.05 (highlighted in blue+red). Of those, 42 miRNAs were up-regulated with adj.p-value < 0.05 (highlighted in red) and 32 miRNAs were down-regulated with adj.p-value < 0.05 (highlighted in blue) in 6 week DMM vs sham.

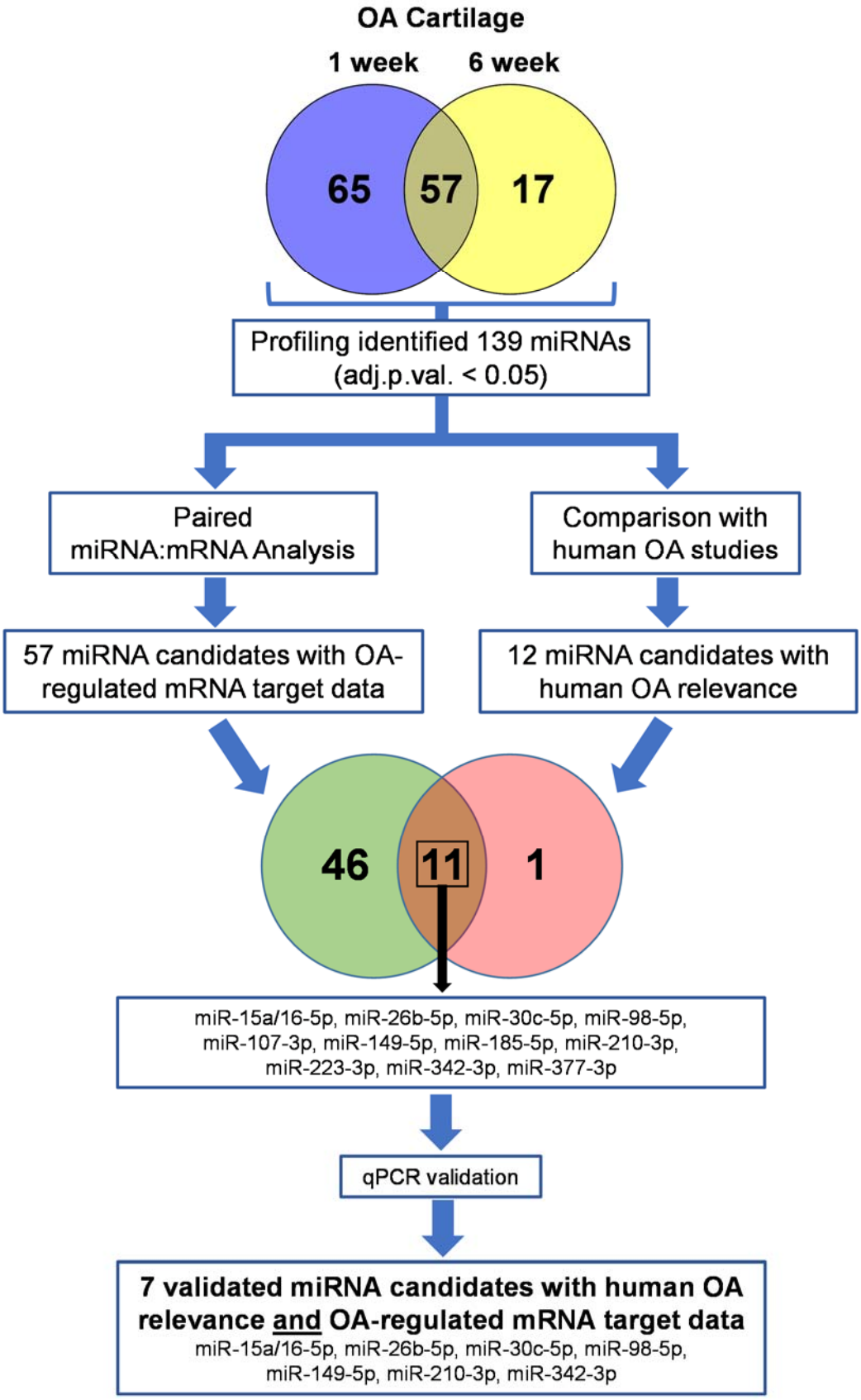

Figure 3. Candidate miRNA filtering strategy. Statistically significant miRNAs dysregulated in either 1 and/or 6 weeks DMM compared with sham (139 miRNAs in total) were filtered based on their paired mRNA target analysis and their overlap with current OA patient data. miRNAs candidates with human OA relevance and OA-regulated mRNA target data were verified with qPCR.

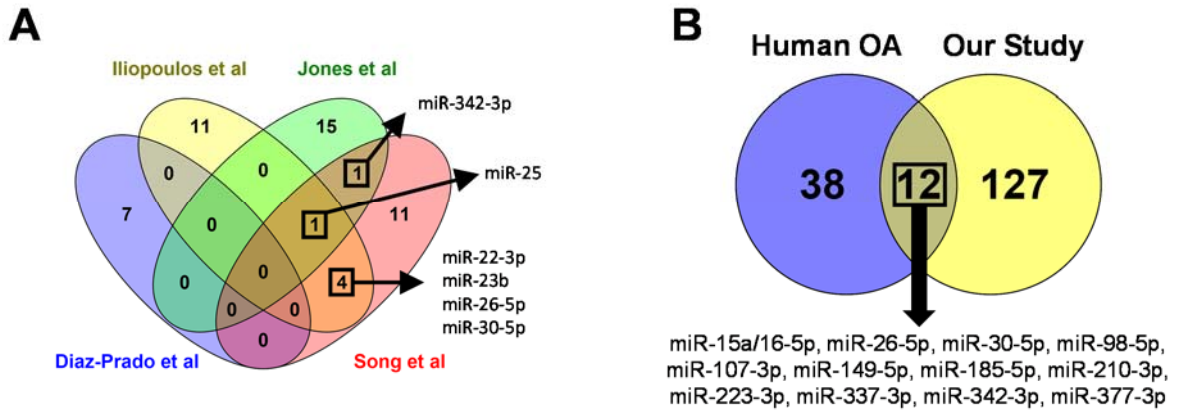

Figure 4. miRNA expression meta-analysis comparing the amount of overlap between previously published human OA studies and our study. **(A)** Differentially expressed miRNAs identified from 4 independent studies examining end-stage human OA cartilage were compared against one another. **(B)** Comparison between the previously published 50 dysregulated miRNAs in human OA and our microarray data demonstrates an overlap of 12 miRNAs common between human end stage OA and mouse early OA cartilage**.**

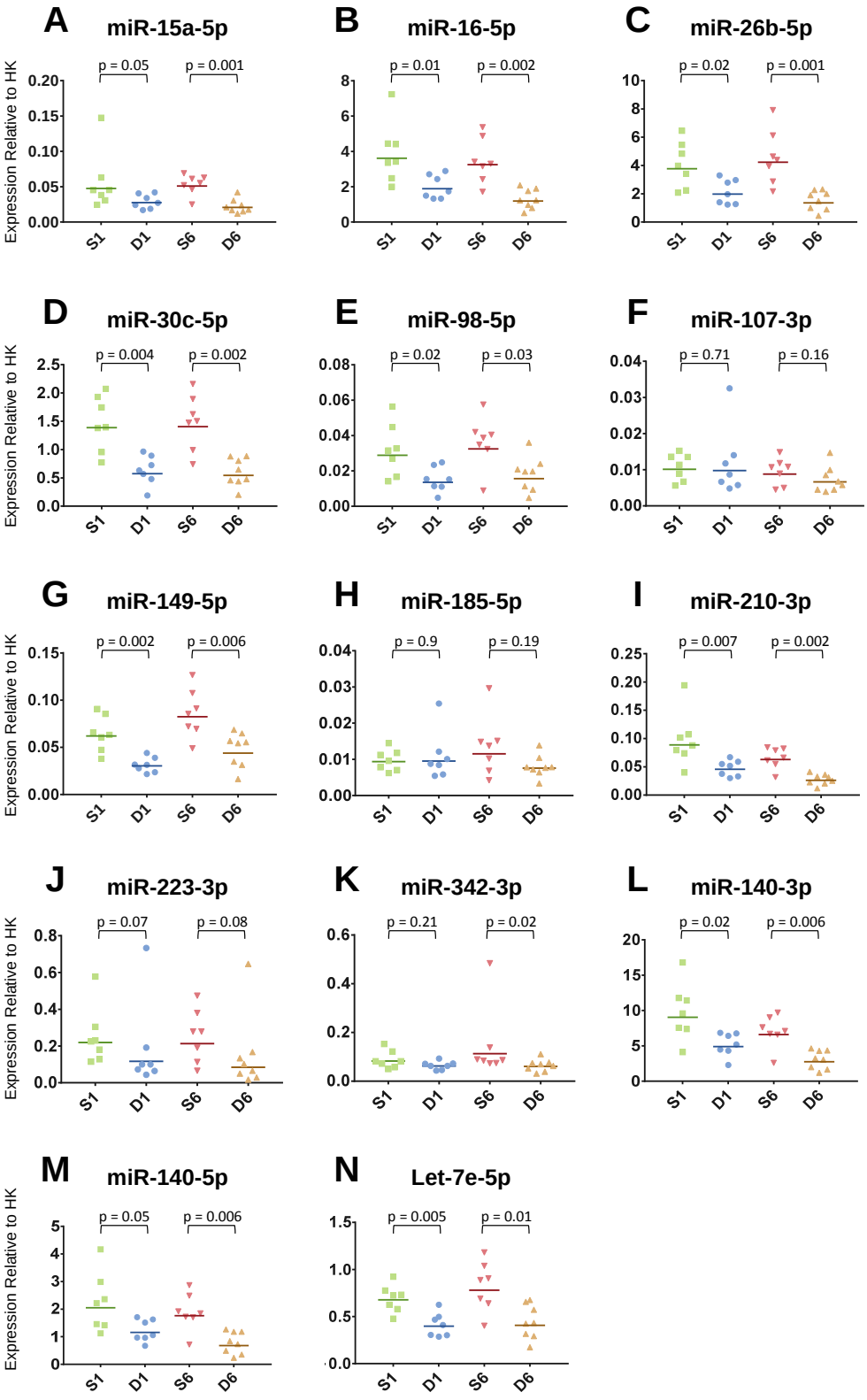

Figure 5. Validation of miRNA expression by qPCR. Expression of miRNAs in articular cartilage tissue from wild type mice at 1 and 6 weeks post sham or DMM surgery was determined. Data shown as expression relative to the average expression of two housekeepers (HK). Each symbol represents an individual mouse (average of 2 technical replicates). Horizontal bars show the geometric mean expression (n=7-8/surgery/timepoint). Statistical differences as determined by Mann-Whitney U test between groups connected by lines with exact p-values for each comparison indicated above the line. S = Sham; D = DMM.

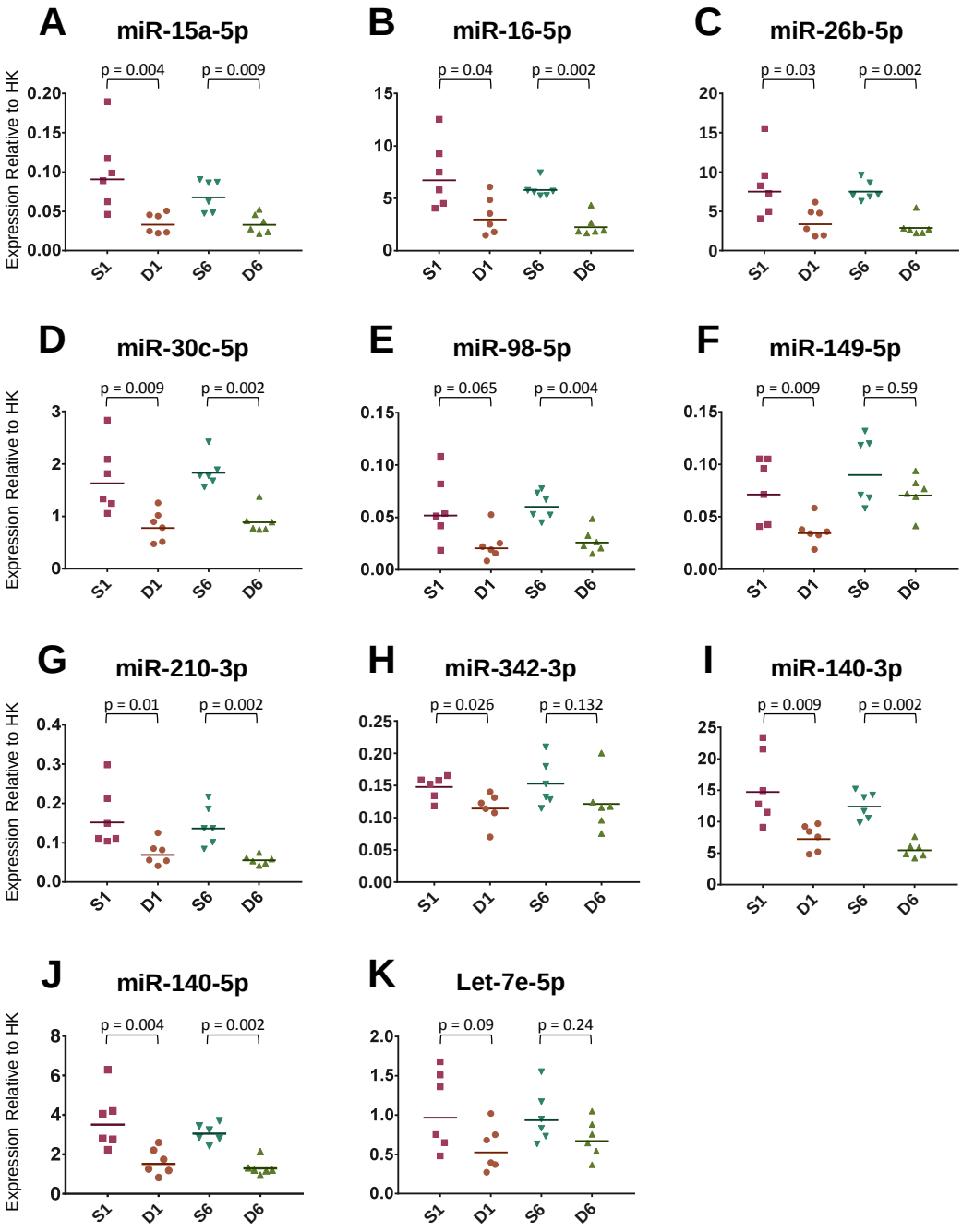

Figure 6. qPCR analysis of miRNA candidates in mice resistant to aggrecan breakdown (Jaffa). Expression of miRNAs in cartilage from Jaffa mice at 1 and 6 weeks post sham or DMM surgery was determined. Data shown as expression relative to the average expression of two housekeepers (HK). Each symbol represents an individual mouse (average of 2 technical replicates). Horizontal bars show the geometric mean expression (n=6/surgery/timepoint). Statistical differences as determined by Mann-Whitney U test between groups connected by lines with exact p-values for each comparison indicated above the line. S = Sham; D = DMM.

Table 1. IPA miRNA target filter analysis on paired miRNA:mRNA expression data in 1 week DMM

miRNA	Fold Change	Source	Confidence	Target Gene	Fold Change	Target Gene Function
mmu-miR-149-5p	-1.24	TargetScan Human	High (predicted)	LTBP2	4.793	Component of TGFβ latent complex, structural component of microfibrils, cell adhesion role
		TargetScan Human	High (predicted)	DLL1	5.359	Notch Delta ligand, mediates cell fate decisions, role in cell-to-cell communications
		TargetScan Human	Moderate (predicted)	TNFRSF12A	5.946	Tumor Necrosis Factor Receptor, weak inducer of apoptosis, cellular adhesion to ECM
		TargetScan Human	Moderate (predicted)	NPR3	7.306	Natriuretic peptide receptor 3, clears C-type Natriuretic Peptide (regulator of cartilage homeostasis)
		TargetScan Human	High (predicted)	IL11	22.880	Cytokine stimulates T-cell-dependent development of Ig-producing B cells, proliferation of hematopoietic stem cells and platelet production
mmu-miR-98-5p	-1.41	TargetScan Human	High (predicted)	NGF	4.807	Nerve growth factor, important in the regulation of growth and differentiation of sympathetic and sensory neurons
		TargetScan Human	High (predicted)	CHSY3	6.220	Chondroitin sulphate synthase 3; Glycosyltransferase enzyme
		TarBase	Experimentally Observed	PTGS2	19.160	Involved in prostaglandin biosynthesis – a major catabolic and inflammatory mediator of cartilage degradation
mmu-miR-26b-5p	-1.27	TargetScan Human	High (predicted)	ZNF385B	5.404	Zinc finger protein, possible role in p53/TP53-mediated apoptosis
		TargetScan Human	High (predicted)	COL10A1	9.680	Chondrocyte hypertrophy
		Ingenuity Expert Findings,Target Scan Human	Experimentally Observed,High (predicted)	PTGS2	19.160	Involved in prostaglandin biosynthesis – a major catabolic and inflammatory mediator of cartilage degradation
mmu-miR-30c-5p	-1.46	TargetScan Human	High (predicted)	BMP7	4.864	TGFβ signalling, plays a role in bone and cartilage development
		TargetScan Human	High (predicted)	ERRFI1	6	Neuregulin signalling
		TarBase	Experimentally Observed	NPR3	7.306	Natriuretic peptide receptor 3, clears C-type Natriuretic Peptide (regulator of cartilage homeostasis)
		TarBase,TargetScan Human	Experimentally Observed,High (predicted)	NT5E	14.162	Nucleotidase enzyme, converts extracellular nucleotides to membrane-permeable nucleosides, defects in gene results in calcification of joints and arteries
mmu-miR-377-3p	-1.37	TargetScan Human	Moderate (predicted)	SEMA3E	5.37	Semaphorin, axonal guidance signalling, role in cell signalling, mediates re-organization of the actin cytoskeleton, promotes focal adhesion disassembly and inhibits adhesion to ECM
		TargetScan Human	High (predicted)	NT5E	14.162	Nucleotidase enzyme, converts extracellular nucleotides to membrane-permeable nucleosides, defects in gene results in calcification of joints and arteries

Table 2. IPA miRNA target filter analysis on paired miRNA:mRNA expression data in 6 week DMM

miRNA	Fold Change	Source	Confidence	Target Gene	Fold Change	Target Gene Function
mmu-miR-26b-5p	-1.36	TargetScan Human	High (predicted)	BHLHE40	3.031	Circadian rhythm signalling
		TargetScan Human	High (predicted)	SGMS2	3.85	Sphingomyelin metabolism
		Ingenuity Expert Findings,Target Scan Human	Experimentally Observed,High (predicted)	PTGS2	32.809	Involved in prostaglandin biosynthesis – a major catabolic and inflammatory mediator of cartilage degradation
mmu-miR-15a-5p/ mmu-miR-16-5p	-1.46	TargetScan Human	High (predicted)	SEMA3D	4.093	Axonal guidance signalling
		TargetScan Human	High (predicted)	FGF1	5.095	Roles in cell survival, cell division, angiogenesis, cell differentiation, tissue repair and cell migration
		TargetScan Human	High (predicted)	HSPA4L	5.184	Possible role as a chaperone, protects cells against the harmful effects of aggregated proteins
		TargetScan Human	Moderate (predicted)	ACSBG1	5.491	Long-chain acyl-CoA synthetase activity, mediates activation of long-chain fatty acids for synthesis of cellular lipids and degradation via beta-oxidation
		TargetScan Human	High (predicted)	RARB	5.626	In concert with RARG, RARB is required for skeletal growth, matrix homeostasis and growth plate function
		TarBase	Experimentally Observed	NPR3	9.254	Natriuretic peptide receptor 3, clears C-type Natriuretic Peptide (regulator of cartilage homeostasis)
		TarBase	Experimentally Observed	PTGS2	32.809	Involved in prostaglandin biosynthesis – a major catabolic and inflammatory mediator of cartilage degradation
mmu-let-7d-5p	-1.29	TarBase	Experimentally Observed	PTGS2	32.809	Involved in prostaglandin biosynthesis – a major catabolic and inflammatory mediator of cartilage degradation
mmu-miR-342-3p	-1.49	TargetScan Human	High (predicted)	BMP7	2.39	TGFβ signalling, plays a role in bone and cartilage development
		TargetScan Human	High (predicted)	BMPR2	3.50	Transmembrane serine/threonine kinases, TGFβ signalling
		TargetScan Human	High (predicted)	SGMS2	3.85	Sphingomyelin metabolism
		TargetScan Human	High (predicted)	PDGFRA	4.314	Tyrosine kinase receptor for PDGF family, role in differentiation of MSC, normal skeletal development, cell proliferation and survival
		TargetScan Human	Moderate (predicted)	IL11	12.389	Cytokine stimulates T-cell-dependent development of Ig-producing B cells, proliferation of hematopoietic stem cells and platelet production
mmu-miR-377-3p	-1.34	TargetScan Human	High (predicted)	SEMA3D	4.09	Semaphorin, Axonal guidance signalling
		TargetScan Human	High (predicted)	PDGFRA	4.314	Tyrosine kinase receptor for PDGF family, role in differentiation of MSC, normal skeletal development, cell proliferation and survival
		TargetScan Human	Moderate (predicted)	SEMA3E	4.494	Semaphorin, axonal guidance signalling, role in cell signalling, mediates re-organization of the actin cytoskeleton, promotes focal adhesion disassembly and inhibits adhesion to ECM
		TargetScan Human	High (predicted)	NT5E	5.649	Nucleotidase enzyme, converts extracellular nucleotides to membrane-permeable nucleosides, defects in gene results in calcification of joints and arteries

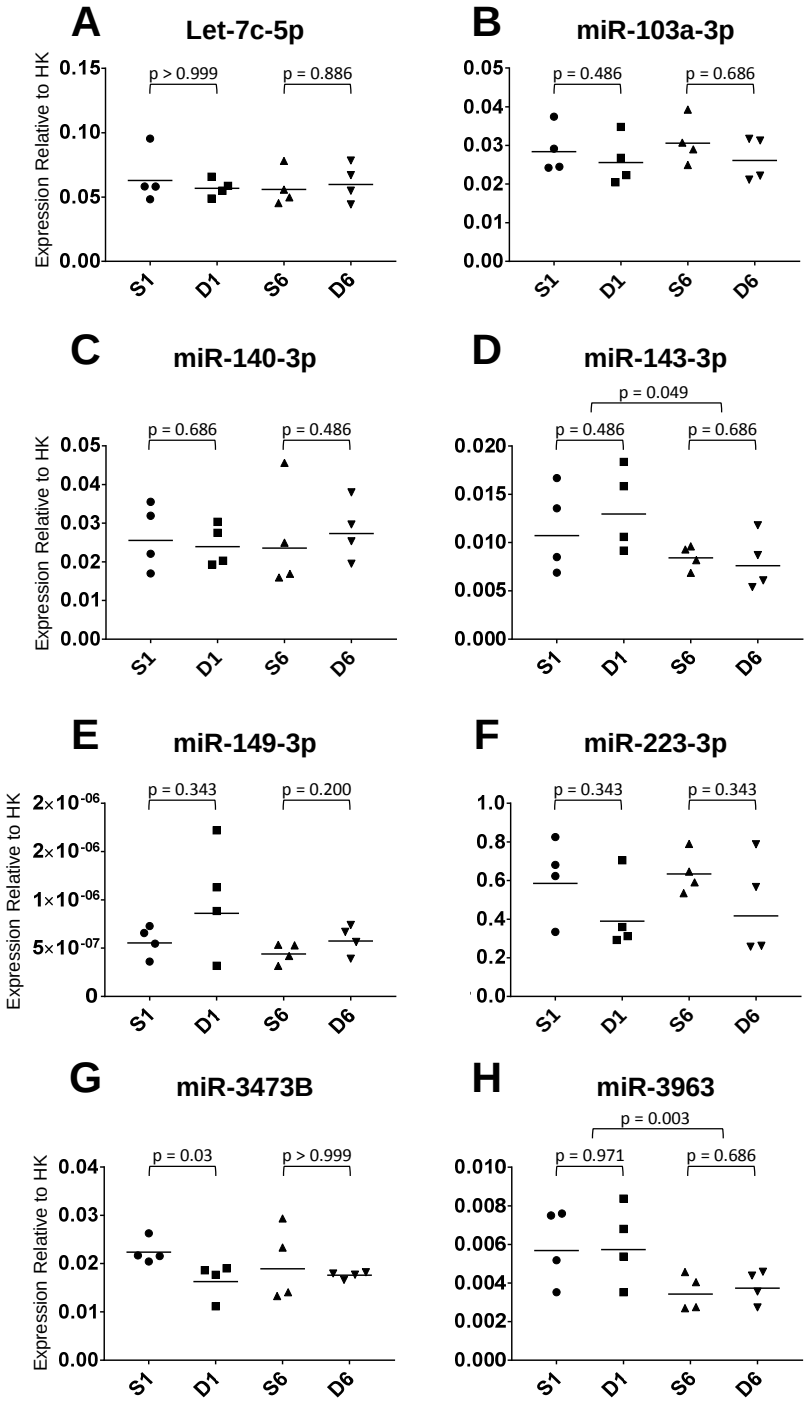

Supplementary Figure 1. Validation of miRNA expression in SCB tissue by qPCR. Expression of miRNAs in SCB tissue from wild type mice at 1 and 6 weeks post sham or DMM surgery was determined. Data shown as expression relative to the average expression of two housekeepers (HK), U6 and 5s. Each symbol represents an individual mouse (average of 2 technical replicates). Horizontal bars show the geometric mean expression (n=4/surgery/timepoint). Statistical differences were determined by unpaired Mann-Whitney U-test between groups connected by lines with exact p-values for each comparison indicated above the line. S = Sham; D = DMM.

Supplemental Table 1: miRNA expression between 6 and 1 week SCB samples

miRBase Accession No.	miRNA	Log_2FC	Average Expression	adj.p.val
MIMAT0025580	mmu-let-7k	1.107576	6.329249031	0.048345
MIMAT0005837	mmu-miR-1187	2.303588	10.31204489	0.048345
MIMAT0000135	mmu-miR-125a-5p	-1.27679	7.109996355	0.048345
MIMAT0000144	mmu-miR-132-3p	-1.32647	5.567654534	0.048345
MIMAT0000219	mmu-miR-24-3p	-1.04639	9.817406411	0.048345
MIMAT0000372	mmu-miR-294-3p	1.391675	6.975797863	0.048345
MIMAT0014834	mmu-miR-3064-5p	0.97805	5.759112855	0.048345
MIMAT0014872	mmu-miR-3082-5p	2.248316	10.52767019	0.048345
MIMAT0014915	mmu-miR-3097-5p	1.04269	5.869133508	0.048345
MIMAT0017050	mmu-miR-32-3p	2.048853	8.492113074	0.048345
MIMAT0003151	mmu-miR-378a-3p	-1.71954	7.459251153	0.048345
MIMAT0019348	mmu-miR-378b	-1.65188	6.585854556	0.048345
MIMAT0025167	mmu-miR-378d	-1.53765	7.247627935	0.048345
MIMAT0004877	mmu-miR-466c-5p	1.283009	6.568837471	0.048345
MIMAT0004881	mmu-miR-466f-5p	1.115477	6.333138133	0.048345
MIMAT0017325	mmu-miR-466i-5p	2.148484	12.33016911	0.048345
MIMAT0005848	mmu-miR-466j	1.559032	7.173326751	0.048345
MIMAT0014891	mmu-miR-466p-5p	0.998899	5.655569582	0.048345
MIMAT0002109	mmu-miR-468-3p	2.015062	8.530434909	0.048345
MIMAT0003130	mmu-miR-486a-5p	1.641124	8.349578463	0.048345
MIMAT0003169	mmu-miR-539-5p	1.087702	6.20791833	0.048345
MIMAT0027104	mmu-miR-5709-3p	0.970164	5.86252855	0.048345
MIMAT0004893	mmu-miR-574-5p	2.197967	11.01195129	0.048345
MIMAT0025162	mmu-miR-6409	0.890151	5.841494934	0.048345
MIMAT0003476	mmu-miR-669b-5p	1.365937	7.006817146	0.048345
MIMAT0005853	mmu-miR-669e-5p	1.663351	7.407783791	0.048345
MIMAT0005839	mmu-miR-669f-3p	-1.21752	5.794922589	0.048345
MIMAT0017323	mmu-miR-669k-5p	1.533465	7.082429704	0.048345
MIMAT0009418	mmu-miR-669l-5p	1.725445	7.804460736	0.048345
MIMAT0009427	mmu-miR-669n	2.084354	9.462586022	0.048345
MIMAT0009421	mmu-miR-669o-5p	1.405256	6.914870044	0.048345
MIMAT0003741	mmu-miR-674-3p	-1.41652	5.909995433	0.048345
MIMAT0027708	mmu-miR-6904-5p	1.374961	6.314877415	0.048345
MIMAT0027736	mmu-miR-6918-5p	1.608301	6.854047821	0.048345
MIMAT0029885	mmu-miR-7682-3p	1.364131	6.366851283	0.048345
MIMAT0000239	mmu-miR-206-3p	1.174687	6.369408784	0.049959
MIMAT0025091	mmu-miR-6348	1.821852	7.926705971	0.049959

Supplemental Table 2. miRNAs dysregulated in 1 week wild-type DMM articular cartilage

miRBase Accession Number	miRNA	Log_2FC	adj.p.val
MIMAT0027762	mmu-miR-6931-5p	2.59	1.23E-05
MIMAT0005837	mmu-miR-1187	1.92	0.000225
MIMAT0014872	mmu-miR-3082-5p	1.85	0.000225
MIMAT0004893	mmu-miR-574-5p	1.82	0.000157
MIMAT0017325	mmu-miR-466i-5p	1.81	0.000134
MIMAT0009427	mmu-miR-669n	1.60	0.001078
MIMAT0002109	mmu-miR-468-3p	1.48	0.001792
MIMAT0017050	mmu-miR-32-3p	1.46	0.002313
MIMAT0009418	mmu-miR-669l-5p	1.31	0.001987
MIMAT0014882	mmu-miR-466m-5p	1.20	0.002313
MIMAT0005853	mmu-miR-669e-5p	1.14	0.00269
MIMAT0025091	mmu-miR-6348	1.14	0.007219
MIMAT0027736	mmu-miR-6918-5p	1.13	0.009616
MIMAT0003735	mmu-miR-672-5p	1.12	0.005016
MIMAT0004881	mmu-miR-466f-5p	1.00	0.002313
MIMAT0009421	mmu-miR-669o-5p	0.99	0.002313
MIMAT0004884	mmu-miR-466h-5p	0.99	0.004174
MIMAT0005848	mmu-miR-466j	0.98	0.002724
MIMAT0003476	mmu-miR-669b-5p	0.97	0.002313
MIMAT0004877	mmu-miR-466c-5p	0.90	0.002724
MIMAT0004885	mmu-miR-467c-5p	0.89	0.004434
MIMAT0000538	mmu-miR-31-5p	0.89	0.010096
MIMAT0017327	mmu-miR-669f-5p	0.85	0.002724
MIMAT0020637	mmu-miR-5126	0.81	0.001792
MIMAT0017000	mmu-miR-195a-3p	0.80	0.008086
MIMAT0027708	mmu-miR-6904-5p	0.80	0.012417
MIMAT0017323	mmu-miR-669k-5p	0.78	0.009616
MIMAT0029885	mmu-miR-7682-3p	0.77	0.018268
MIMAT0019336	mmu-miR-3960	0.76	0.002313
MIMAT0028133	mmu-miR-7118-5p	0.75	0.002313
MIMAT0028404	mmu-miR-7218-5p	0.75	0.023742
MIMAT0029792	mmu-miR-6546-5p	0.72	0.008086
MIMAT0017277	mmu-miR-504-3p	0.70	0.02205
MIMAT0027818	mmu-miR-6959-5p	0.68	0.009616
MIMAT0004625	mmu-miR-16-1-3p	0.66	0.005798
MIMAT0031416	mmu-miR-8110	0.65	0.002313
MIMAT0031396	mmu-miR-8095	0.65	0.020412
MIMAT0028040	mmu-miR-6769b-5p	0.63	0.006168
MIMAT0027964	mmu-miR-7030-5p	0.61	0.009684
MIMAT0028071	mmu-miR-7082-3p	0.61	0.02153
MIMAT0007867	mmu-miR-1895	0.60	0.012379
MIMAT0004865	mmu-miR-297c-5p	0.59	0.009616
MIMAT0027980	mmu-miR-7038-5p	0.58	0.010096
MIMAT0014922	mmu-miR-3101-3p	0.58	0.002724
MIMAT0009390	mmu-miR-1927	0.57	0.049018
MIMAT0025123	mmu-let-7j	0.55	0.017533

MIMAT0017340	mmu-miR-1930-3p	0.55	0.018824
MIMAT0017254	mmu-miR-499-3p	0.55	0.010096
MIMAT0029862	mmu-miR-129b-5p	0.55	0.046369
MIMAT0000239	mmu-miR-206-3p	0.53	0.010656
MIMAT0004664	mmu-miR-214-5p	0.53	0.014219
MIMAT0000670	mmu-miR-222-3p	0.52	0.010656
MIMAT0005460	mmu-miR-1224-5p	0.52	0.004434
MIMAT0009411	mmu-miR-1306-3p	0.51	0.004464
MIMAT0017256	mmu-miR-700-5p	0.49	0.012417
MIMAT0000372	mmu-miR-294-3p	0.47	0.049018
MIMAT0004624	mmu-miR-15a-3p	0.47	0.020412
MIMAT0022372	mmu-miR-5622-3p	0.46	0.049857
MIMAT0014918	mmu-miR-3098-3p	0.44	0.010096
MIMAT0020606	mmu-miR-5099	0.41	0.042116
MIMAT0000597	mmu-miR-346-5p	0.40	0.018824
MIMAT0027972	mmu-miR-7034-5p	0.40	0.010656
MIMAT0017018	mmu-miR-16-2-3p	0.39	0.040445
MIMAT0003483	mmu-miR-696	0.39	0.047519
MIMAT0004525	mmu-miR-99b-3p	0.33	0.049018
MIMAT0025583	mmu-miR-6538	0.33	0.029771
MIMAT0027940	mmu-miR-7018-5p	0.33	0.042116
MIMAT0027976	mmu-miR-7036a-5p	0.31	0.032763
MIMAT0007864	mmu-miR-1897-5p	0.31	0.049857
MIMAT0000159	mmu-miR-149-5p	-0.31	0.049018
MIMAT0000131	mmu-miR-99a-5p	-0.33	0.030866
MIMAT0000658	mmu-miR-210-3p	-0.33	0.049018
MIMAT0000534	mmu-miR-26b-5p	-0.34	0.025267
MIMAT0000571	mmu-miR-331-3p	-0.35	0.023711
MIMAT0004523	mmu-miR-29b-1-5p	-0.35	0.049008
MIMAT0000248	mmu-miR-30e-5p	-0.37	0.033661
MIMAT0004632	mmu-miR-29c-5p	-0.37	0.018824
MIMAT0000140	mmu-miR-128-3p	-0.38	0.018684
MIMAT0000580	mmu-miR-148b-3p	-0.39	0.018824
MIMAT0000148	mmu-miR-136-5p	-0.39	0.023742
MIMAT0000578	mmu-miR-337-3p	-0.39	0.049383
MIMAT0000525	mmu-let-7f-5p	-0.39	0.049857
MIMAT0004536	mmu-miR-151-5p	-0.40	0.012379
MIMAT0004629	mmu-miR-22-5p	-0.40	0.019218
MIMAT0027846	mmu-miR-6972-5p	-0.40	0.016659
MIMAT0003485	mmu-miR-455-5p	-0.40	0.045711
MIMAT0019349	mmu-miR-101c	-0.41	0.025368
MIMAT0003456	mmu-miR-495-3p	-0.41	0.014219
MIMAT0019339	mmu-miR-28c	-0.41	0.014219
MIMAT0001421	mmu-miR-434-5p	-0.42	0.02511
MIMAT0000653	mmu-miR-28a-5p	-0.43	0.008086
MIMAT0000567	mmu-miR-329-3p	-0.45	0.041474
MIMAT0000660	mmu-miR-181a-1-3p	-0.45	0.004646
MIMAT0000674	mmu-miR-181c-5p	-0.45	0.008086
MIMAT0000518	mmu-miR-196a-5p	-0.45	0.018824
MIMAT0000129	mmu-miR-30a-3p	-0.46	0.012417

MIMAT0000522	mmu-let-7b-5p	-0.46	0.012417
MIMAT0000741	mmu-miR-377-3p	-0.46	0.019218
MIMAT0000671	mmu-miR-224-5p	-0.46	0.012417
MIMAT0000521	mmu-let-7a-5p	-0.46	0.018824
MIMAT0004644	mmu-miR-337-5p	-0.46	0.018961
MIMAT0009456	mmu-miR-1839-5p	-0.47	0.013899
MIMAT0000249	mmu-miR-30e-3p	-0.47	0.010096
MIMAT0003388	mmu-miR-376b-5p	-0.47	0.010525
MIMAT0000704	mmu-miR-361-5p	-0.47	0.012379
MIMAT0000523	mmu-let-7c-5p	-0.48	0.010096
MIMAT0004883	mmu-miR-466g	-0.48	0.020412
MIMAT0004747	mmu-miR-411-5p	-0.49	0.017533
MIMAT0000545	mmu-miR-98-5p	-0.49	0.008086
MIMAT0000743	mmu-miR-379-5p	-0.50	0.023711
MIMAT0004750	mmu-miR-425-5p	-0.51	0.008086
MIMAT0005839	mmu-miR-669f-3p	-0.53	0.022212
MIMAT0017080	mmu-miR-379-3p	-0.53	0.005066
MIMAT0004882	mmu-miR-466f-3p	-0.53	0.031566
MIMAT0003183	mmu-miR-376c-3p	-0.53	0.010096
MIMAT0022836	mmu-miR-299b-5p	-0.53	0.020412
MIMAT0000514	mmu-miR-30c-5p	-0.54	0.014219
MIMAT0005834	mmu-miR-466i-3p	-0.54	0.045711
MIMAT0014953	mmu-miR-374c-5p	-0.56	0.003005
MIMAT0001093	mmu-miR-411-3p	-0.58	0.012409
MIMAT0001081	mmu-miR-196b-5p	-0.59	0.002724
MIMAT0027808	mmu-miR-6954-5p	-0.61	0.047581

Supplemental Table 3. miRNAs dysregulated in 6 week wild-type DMM articular cartilage

miRBase Accession Number	miRNA	Log_2FC	adj.p.val
MIMAT0027762	mmu-miR-6931-5p	1.76	0.00040919
MIMAT0020606	mmu-miR-5099	1.47	6.30E-05
MIMAT0005837	mmu-miR-1187	1.42	0.003098
MIMAT0014872	mmu-miR-3082-5p	1.39	0.003098
MIMAT0004893	mmu-miR-574-5p	1.30	0.003098
MIMAT0017050	mmu-miR-32-3p	1.30	0.00642743
MIMAT0009427	mmu-miR-669n	1.30	0.00642743
MIMAT0017325	mmu-miR-466i-5p	1.30	0.00274162
MIMAT0002109	mmu-miR-468-3p	1.25	0.00642743
MIMAT0009418	mmu-miR-669l-5p	1.14	0.00642743
MIMAT0014882	mmu-miR-466m-5p	1.06	0.00665187
MIMAT0005853	mmu-miR-669e-5p	1.05	0.00642743
MIMAT0003735	mmu-miR-672-5p	1.00	0.01201088
MIMAT0025091	mmu-miR-6348	0.98	0.01863644
MIMAT0027736	mmu-miR-6918-5p	0.93	0.03030302
MIMAT0004881	mmu-miR-466f-5p	0.88	0.00665187
MIMAT0004884	mmu-miR-466h-5p	0.86	0.01190543
MIMAT0005848	mmu-miR-466j	0.86	0.00967734
MIMAT0003476	mmu-miR-669b-5p	0.85	0.00665187
MIMAT0004885	mmu-miR-467c-5p	0.85	0.00878541
MIMAT0000538	mmu-miR-31-5p	0.85	0.01829985
MIMAT0009421	mmu-miR-669o-5p	0.79	0.00985442
MIMAT0017000	mmu-miR-195a-3p	0.77	0.01302404
MIMAT0004877	mmu-miR-466c-5p	0.77	0.00997571
MIMAT0017327	mmu-miR-669f-5p	0.72	0.00967734
MIMAT0017323	mmu-miR-669k-5p	0.67	0.02596135
MIMAT0028133	mmu-miR-7118-5p	0.66	0.00642743
MIMAT0027708	mmu-miR-6904-5p	0.64	0.04642232
MIMAT0004625	mmu-miR-16-1-3p	0.56	0.01790053
MIMAT0028071	mmu-miR-7082-3p	0.55	0.0472076
MIMAT0014922	mmu-miR-3101-3p	0.55	0.00642743
MIMAT0000239	mmu-miR-206-3p	0.53	0.01664266
MIMAT0027980	mmu-miR-7038-5p	0.52	0.02501045
MIMAT0027964	mmu-miR-7030-5p	0.50	0.03091367
MIMAT0014918	mmu-miR-3098-3p	0.48	0.01158572
MIMAT0025123	mmu-let-7j	0.47	0.04648128
MIMAT0009411	mmu-miR-1306-3p	0.47	0.00985442
MIMAT0000597	mmu-miR-346-5p	0.46	0.01550893
MIMAT0004865	mmu-miR-297c-5p	0.46	0.04136029
MIMAT0004624	mmu-miR-15a-3p	0.46	0.03649558
MIMAT0015640	mmu-miR-3470a	0.45	0.03199237
MIMAT0017256	mmu-miR-700-5p	0.41	0.04248872
MIMAT0001081	mmu-miR-196b-5p	-0.34	0.04642232
MIMAT0000383	mmu-let-7d-5p	-0.37	0.03985318
MIMAT0000653	mmu-miR-28a-5p	-0.37	0.0208685
MIMAT0003388	mmu-miR-376b-5p	-0.39	0.0375765

MIMAT0000140	mmu-miR-128-3p	-0.39	0.02235794
MIMAT0019339	mmu-miR-28c	-0.40	0.02610626
MIMAT0003183	mmu-miR-376c-3p	-0.40	0.04642232
MIMAT0000741	mmu-miR-377-3p	-0.43	0.04136029
MIMAT0017080	mmu-miR-379-3p	-0.43	0.01829985
MIMAT0004536	mmu-miR-151-5p	-0.43	0.01201088
MIMAT0000148	mmu-miR-136-5p	-0.44	0.02199432
MIMAT0000534	mmu-miR-26b-5p	-0.44	0.01302404
MIMAT0000648	mmu-miR-10a-5p	-0.45	0.02596135
MIMAT0000378	mmu-miR-300-3p	-0.46	0.04136029
MIMAT0001093	mmu-miR-411-3p	-0.46	0.04642232
MIMAT0004691	mmu-miR-382-3p	-0.47	0.02135542
MIMAT0000214	mmu-miR-185-5p	-0.47	0.04642232
MIMAT0022836	mmu-miR-299b-5p	-0.48	0.04642232
MIMAT0000567	mmu-miR-329-3p	-0.49	0.04248872
MIMAT0000164	mmu-miR-154-5p	-0.49	0.03199237
MIMAT0009456	mmu-miR-1839-5p	-0.50	0.01639113
MIMAT0003130	mmu-miR-486a-5p	-0.50	0.02833464
MIMAT0000655	mmu-miR-100-5p	-0.51	0.02883388
MIMAT0000124	mmu-miR-15b-5p	-0.54	0.01179409
MIMAT0000526	mmu-miR-15a-5p	-0.55	0.01201088
MIMAT0000590	mmu-miR-342-3p	-0.57	0.01717305
MIMAT0000658	mmu-miR-210-3p	-0.59	0.00661549
MIMAT0000647	mmu-miR-107-3p	-0.62	0.00642743
MIMAT0001422	mmu-miR-434-3p	-0.62	0.02199432
MIMAT0000544	mmu-miR-129-2-3p	-0.62	0.00642743
MIMAT0000665	mmu-miR-223-3p	-1.19	0.04648128
MIMAT0001632	mmu-miR-451a	-1.34	0.04648128